Carbon Isotope Stratigraphy of the late Proterozoic Wonoka Formation of the Adelaide Fold Belt: Diagenetic Assessment and Interpretation of Isotopic Signature and Correlations with Previously Measured Isotopic Curves

BEN URLWIN B.Sc.

Department of Geology and Geophysics

University of Adelaide

November, 1992

Thesis submitted as partial fulfilment of the requirements

for the Honours Degree of Bachelor of Science.

National Grid Reference:

COPLEY 1:250,000

SH 54-9 6636

ABSTRACT

The Wonoka Formation of the Adelaide Fold Belt represents the only well-described example of a late Proterozoic storm dominated carbonate shelf sequence with the considerable thickness and lateral extent of the formation making it an excellent opportunity for applying the principles of isotope stratigraphy. Sequences exposed at Warraweena, which lies on the boundary between the Central and Northern Flinders Zones, were analysed for stable isotope ratios of carbon and oxygen.

Geochemical, petrographic and cathodoluminescent analysis of individual samples was used to identify those carbonates which have experienced significant diagenetic alteration. These values were not included in the interpretation of the formation's isotopic signal.

Plotting of the least altered values against stratigraphic height revealed a consistent carbon isotopic trend. This trend was divided into two sections, termed the Lower Wonoka Signal and the Upper Wonoka Signal. The Lower Wonoka Signal is defined by the extremely consistent negative signal ($\partial^{13}C$ = -8 to -7 ‰) characteristic of the lower- to mid-Wonoka Formation. This signal is interpreted to be a product of deposition and lithification in basinal waters that contain anomalously light dissolved carbonate. The Upper Wonoka Signal comprises a shift to more positive values ($\partial^{13}C$ = -5 to +6 ‰) and is interpreted to be a reflection of carbonate deposition in shallow surface waters, possibly in association with the formation of a partially restricted lagoon.

Strontium isotopic analysis reveals $^{87}Sr/^{86}Sr$ values that are interpreted to be of primary origin. These values, when compared to data obtained by previous authors for the equivalent time period, give an estimated age of 560-590 Ma for the Wonoka Formation.

Table of Contents

List of Figures

List of Plates

List of Tables

List of Appendices

CHAPTER 1 INTRODUCTION

1.1 Preamble

Increased understanding of the fractionation processes acting in carbonate systems has facilitated the use of carbon and oxygen isotopes in correlating sedimentary sequences which lack appropriate biostratigraphic controls (Anderson and Arthur, 1983; Kroopnick et al., 1977; Berger and Vincent, 1986; Aharon et al., 1987; Jansen, 1989).

Oxygen isotope data can provide information on changes in the temperature of the ocean that have occured throughout geological history, whereas stratigraphic variations in the carbon isotopic signal reflect disturbances in the carbon cycle that can be linked to changes in organic matter productivity and burial (Marshall, 1991). Carbon isotopes, being relatively unaffected by temperature variations, provide an excellent stratigraphic tool for both inter- and intra- basinal correlations. Variations in the isotopic composition of sea water over geological time may be recorded in the carbonate rocks present in the sedimentary record. Such secular variations have proven to be an extremely useful tool in the correlation of Phanerozoic successions (Berger and Vincent, 1986; Jansen, 1989; Magaritz, 1989, 1990). It has not been until relatively recently, however, that the potential of carbon isotope stratigraphy in the Proterozoic has been realised. Numerous recent works have investigated the global correlation of late Precambrian and Cambrian sequences, especially across the Precambrian/Cambrian boundary where the rapid Cambrian faunal radiation has had a distinctive effect upon the carbon isotopic signal (e.g. Magaritz et al., 1986; Brasier et al., 1990; Tucker, 1990; Kirschvink et al., 1991).

Any search for secular variations in the Precambrian carbon isotopic record needs to take into account the processes that can cause post-depositional (diagenetic) isotopic fractionation. Through the application of petrography, cathodoluminescence (CL), and the use of trace and major element data, these diagenetic processes can be quantified and their effect on the isotopic signal of carbonates evaluated.

In the present study, the principles of carbon isotope stratigraphy are applied to the late Proterozoic Wonoka Formation of the Adelaide Fold Belt. The Wonoka Formation represents the only well-described Proterozoic example of a storm-dominated carbonate

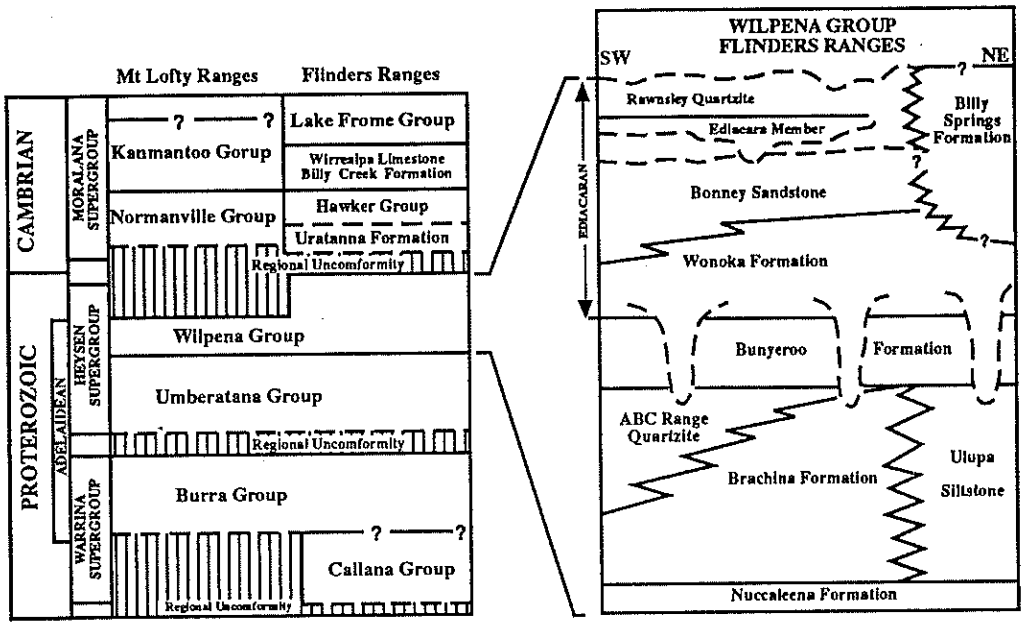

Figure 1.1 Lithostratigraphic subdivisions of the Adelaide Fold Belt, showing detail of the Wilpena Group in the Flinders Ranges (after Preiss, 1987).

shelf sequence, being unique in its considerable thickness and lateral extent, and thus provides an excellent opportunity to produce a complete carbon isotope stratigraphy.

1.2 Geological Setting

The Adelaide Fold Belt comprises a major, north-south trending zone of late Proterozoic to Cambrian sedimentary, metamorphic and igneous rocks. It extends from Kangaroo Island and the Mount Lofty Ranges in the south, through to the Flinders Ranges in the north.

Current theories propose that the Adelaide Fold Belt resembles a passive continental margin setting in the southern Flinders Ranges and an intracontinental rift, or aulacogen, in the central and northern Flinders Ranges (von der Borch, 1980; von der Borch et al., 1982). Another interpretation has related the Adelaide Fold Belt sediments to repeated cycles of lithospheric extension and thermal subsidence (Jenkins, 1990). The Adelaide Geosyncline has been divided into three, unconformity-bound supergroups. These are the Warrina Supergroup (basal) which includes the synrift Callana and Burra Groups; the Heysen Supergroup which includes the glacial and marine sediments of the Umberatana Group and the post-glacial Wilpena Group; and the Moralana Supergroup (uppermost). This study focuses on the Wonoka Formation, which forms part of the uppermost of the two coarsening and shallowing-upward, regressive cycles which characterize the Wilpena Group (Fig. 1.1).

1.3 Location and Local Geology

The Warraweena area is located 35 km south-east of Leigh Creek and 27 km east of Beltana (Figure 1.2). It is situated on the transition between the Central Flinders Zone (CFZ: Preiss, 1987), which is an area of shelfal deposition, and the North Flinders Zone (NFZ) which is of more basinal aspect.

The geology of the Warraweena area is dominated by the Mount Goddard and Mount Hack Synclines, which are separated by a major east-west trending thrust fault (the Warraweena Fault) and the Mount Stuart Anticline (Coats, 1973; Scotford, 1984). Two

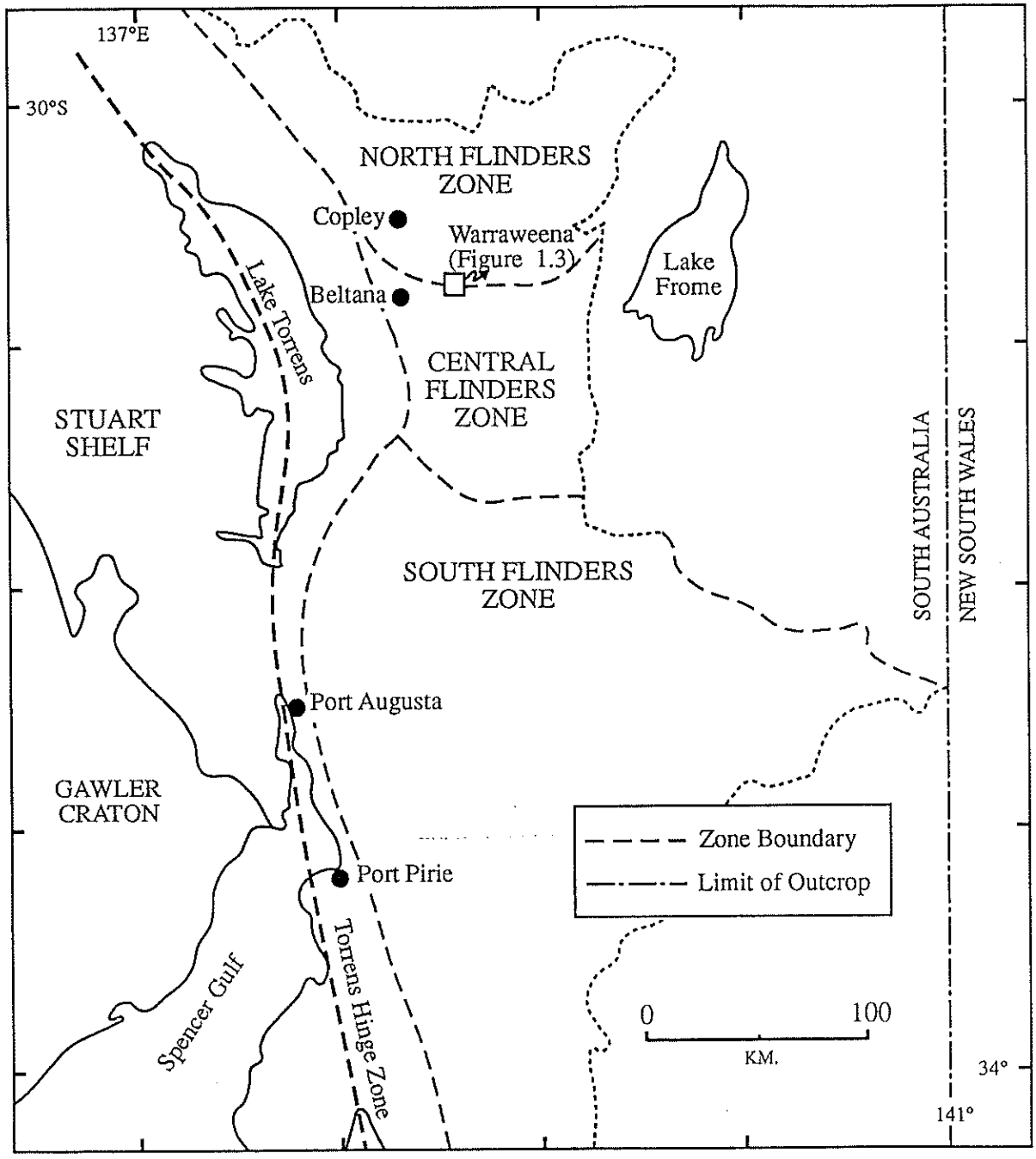

Figure 1.2 Location of study area in the Adelaide Fold Belt. The Warraweena study area is outlined in Figure 1.3 (after Priess et al., 1981).

diapirs, which show evidence of having affected the deposition of the adjacent late Proterozoic sediments, occur in the Warraweena area, one to the south-east and one to the east of the Mount Goddard Syncline (Figure 1.3).

Three sections were measured through the Wonoka Formation within the study area. One was measured on each limb of the Mount Goddard Syncline, and these are referred to as the North Goddard and South Goddard Sections, respectively. A third section was measured at Black Range Springs on the northern limb of the Mount Stuart Anticline (Figure 1.3).

1.4 Previous Investigations

The first descriptions of what is now known as the Wonoka Formation were made by Sir Douglas Mawson, who, between 1923 and 1949, wrote a series of papers detailing the structure and stratigraphy of the Flinders Ranges. Dalgarno and Johnson (1964) formally defined the Wonoka Formation, designating the section exposed at Brachina Gorge as the type section. Gostin and Jenkins (1983) have subsequently redefined the base of the Wonoka Formation, lowering it to the base of a thin, but laterally persistent dolomite horizon (the "Wearing Dolomite Member" of Dalgarno et al., 1964). This redefined boundary, which is equivalent to Haines (1987) Unit 1, is easily mappable and represents a distinct and basinwide lithostrome and sedimentologic change from the Bunyeroo Formation. Newer work by DiBona (1989) and Christie-Blick et al. (1991) suggests that this boundary represents a combined sequence boundary and condensed interval. The former boundary of Dalgarno and Johnson (1964) was generally mapped as the colour change from dominantly maroon to dominantly green shales and, although it was relatively easily detected on black and white aerial photographs, it may be highly gradational and laterally diachronous (Haines, 1987). Even so, some authors still maintain this original definition of the Wonoka Formation (e.g. Preiss, 1987).

Haines (1987) provided one of the first, and most comprehensive, studies of the Wonoka Formation, dividing the section exposed at Bunyeroo Gorge into eleven mappable and lithologically distinct units. These individual units are comparable with the Wonoka Formation as seen in the Central Flinders Ranges, but the uppermost units lose applicability

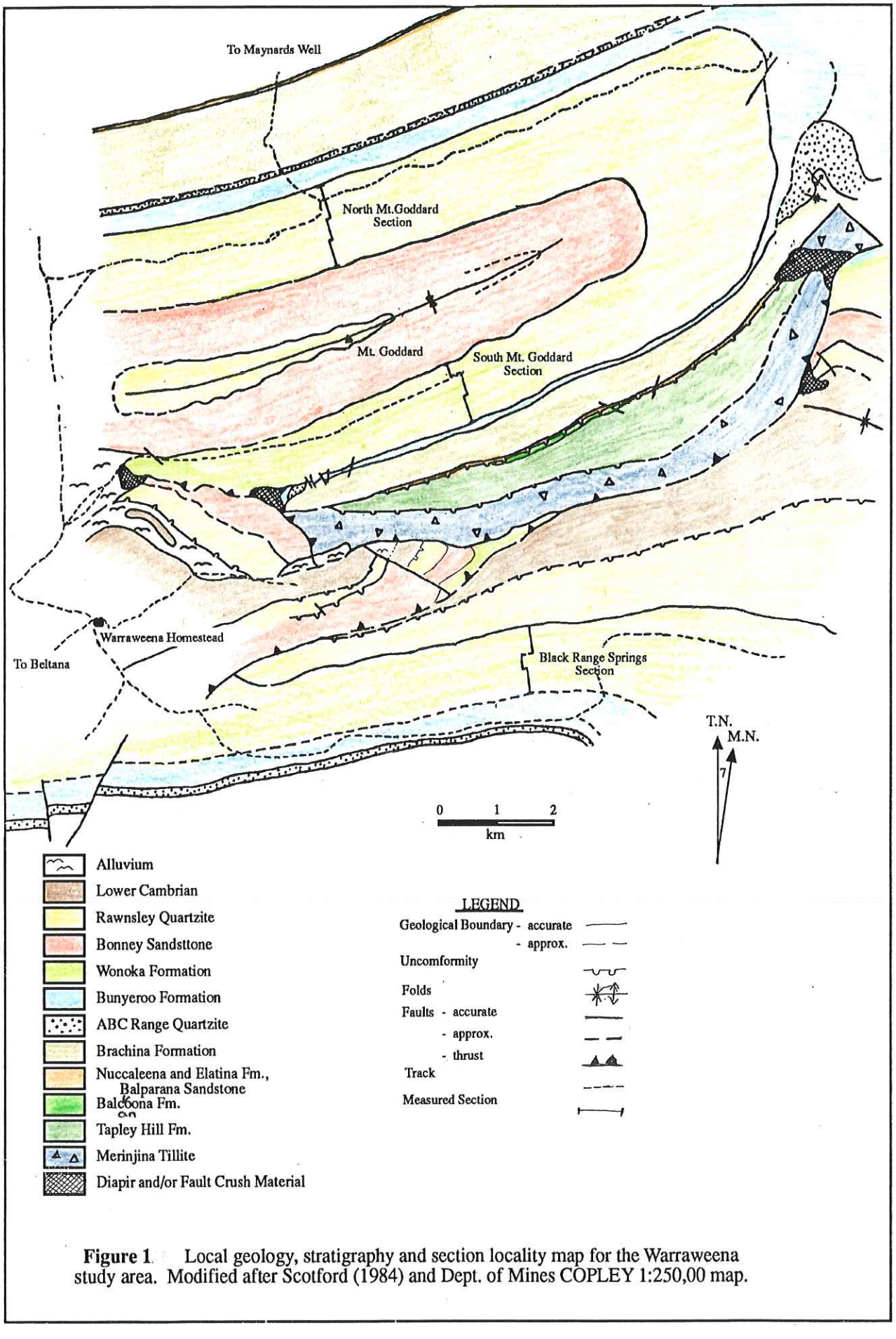

Figure 1 Local geology, stratigraphy and section locality map for the Warraweena study area. Modified after Scotford (1984) and Dept. of Mines COPLEY 1:250,00 map.

in the more northern areas.

DiBona (1989) provided an alternative subdivision of the Wonoka Formation, using the principles of sequence stratigraphy. He divided the formation into nine lithostratigraphic units and four, unconformity-bounded sequences. Throughout the present study Haines' (1987) units and the redefined boundary of Gostin and Jenkins (1983) are used, these being the more widely acknowledged reference terms.

Previous studies of the Wonoka Formation have centred on either the broad sedimentology and stratigraphy of the unit, or its localised deposition in large canyons. Detailed isotopic work has been somewhat limited. Singh (1986) provided the first insight into the isotopic values encoded within the Wonoka carbonates with a petrographic and isotopic study of oolite facies present at the top of the unit. Eickoff et al. (1988) reported isotopic measurements on wall plaster, oolitic limestones and brown dolomite clasts from the Fortress Hill region in the northern Flinders Zone. Jansyn (1990) provided one of the first complete carbon isotope curves for the Wonoka Formation, detailing the section at Bunyeroo Gorge.

This study is directed at furthering our knowledge of the isotope variations recorded within the Wonoka Formation, and at providing some insight into the secondary processes which may have affected these late Proterozoic carbonates.

1.5 Regional Late Proterozoic Stratigraphy

1.5.1 Nuccaleena Formation

The Nuccaleena Formation is a persistent, cream to yellow weathering dolomite that represents a regionally consistent marker horizon. This unit marks the base of the Wilpena Group and is thought to represent a primary micritic dolomite that was depositied in a shallow marine environment (Williams, 1979) very similar to the Wearing Dolomite member of the basal Wonoka Formation. Thin laminae with low angle cross-bedding, stromatolites, teepee structures and intraclast breccias are amongst its sedimentary features (Williams, 1979; Plummer, 1987).

1.5.2 Brachina Formation

The Brachina Formation represents a fining, then coarsening upward, storm-dominated sequence that is composed of a thick succession of brown, greyish red and khaki siltstone (Christie-Blick et al., 1980) with local intercalations of slumped mudstones and fine sandstones (Eickoff et al., 1987). This unit has, in places, been eroded to within 100 m of its base by canyon incision (Eickoff et al., 1987).

1.5.3 ABC Range Quartzite

The ABC Range Quartzite is composed of greyish red to white, coarse- to fine-grained quartzites which are cyclically interstratified with very fine-grained sandstone and siltstone (Christie-Blick et al., 1990). Conglomeratic beds (sedimentary breccias) representing reworking of the sediments have been noted in the Warraweena area and near the Woolshed and Wilpena Faults (Jansyn, 1990) and may be related to fault movements (Scotford, 1984). The unit becomes finer-grained and lenses out towards the north and east, presumably by interfingering with the underlying Brachina Formation (Plummer, 1978; Christie-Blick et al., 1990; Eickoff et al., 1987).

1.5.4 Bunyeroo Formation

The Bunyeroo Formation is composed of red-purple silty shales and, in the northern Flinders Ranges, sharply overlies either the ABC Range Quartzite or the Brachina Formation (von der Borch et al 1988). The unit represents a period of abrupt transgression and/or subsidence (Gostin and Jenkins, 1983). The massive, homogeneous nature of the unit suggests suspension settling of sediment below wave base under low energy, oxidative conditions (Haines, 1987; von der Borch, 1988). Major thickness variations have been noted by various authors (Scotford, 1984; Abbott, 1986; Haines, 1987; Preiss, 1987; DiBona 1989; Christie-Blick et al., 1990) and are thought to relate to salt build-up at depth preventing subsidence of the basin in certain areas (Christie-Blick, 1990). The Bunyeroo Formation also contains the Lake Acraman impact ejecta horizon of Gostin et al. (1986). This horizon is composed of a thin, but very persistent layer of acid to intermediate volcanic fragments (from sand-size to 30 cm blocks) and characteristically occurs 80-90 m above the

base of the Bunyeroo Formation in the western Flinders Ranges.

1.5.5 Wonoka Formation

The Wonoka Formation is a mainly regressive, mixed carbonate/siliciclastic sequence of marine origin. The vertical sequence reflects the gradual development, progradation and eventual destruction of a storm-dominated carbonate ramp, deposited under open shelf conditions (Haines, 1987). The shallowing linked to this cycle culminated with the deposition of lagoonal, tidal and supratidal carbonates and siliciclastics which intertonge with the overlying Bonney Sandstone (Haines, 1987; DiBona, 1989).

Major canyon/channel fill sequences have been observed in the Wonoka Formation by various authors (e.g. Coats, 1964; von der Borch et al., 1982, 1988; Eickhoff et al., 1988; Haines, 1988; DiBona , 1989). Excavated and filled during early Wonoka time, these canyons, in some places, cut down over 1 kilometre into the underlying Bunyeroo Formation and ABC Range Quartzite. The genesis of these canyons is controversial, with alternative subaerial and submarine origins being proposed (von der Borch et al., 1982, 1988; Gostin and Jenkins, 1983; von der Borch and Grady, 1984; Haines, 1986, 1987, 1988; Eickoff et al., 1988; DiBona, 1989; Christie-Blick et al., 1990; Jenkins, 1990).

CHAPTER 2 STRATIGRAPHIC SUBDIVISIONS OF THE WONOKA FORMATION

2.1 Unit 1

In the study area, Unit 1 occurs as a thin, brown, massive dolomite layer averaging approximately 20 to 30 cm in thickness. The layer is obviously cupriferous, with malachite staining visible on most weathered samples. Unit 1 is interpreted here to be deposited in the shallow water, oxidizing environment of a shelf, at a time of low sea level, just below fair weather wave base (Jansyn, 1990; R.J.F. Jenkins, pers. comm.). Unit 1 represents a lowstand systems tract, where the regression apparent at the top of the Bunyeroo Formation ceases, and the transgression evident in Unit 2 begins.

2.2 Unit 2

At the North Mount Goddard locality Unit 2 is seen as a 50 m sequence of alternating brown, fine-grained calcareous and dolomitic sandstone turbidites and coarse siltstone, with maroon calcareous shales. The sandstones are fine-grained and include sedimentary structures such as well-developed flute casts, and both small and large scale, hummocky cross-stratification (HCS) (Haines, 1987; DiBona, 1989). This unit represents a transgressive phase, with the maximum flooding surface occurring at, or near, the top of the unit. Unit 2 was not identified at Black Range Springs section and is absent at South Mount Goddard (Fig. 2.1).

2.3 Unit 3

Unit 3 comprises finely laminated reddish calcareous silty shale, with varying amounts of very thin bedded, pink, micritic to microsparitic limestone. These limestone beds are generally <2 cm thick, and frequently occur in packages of 2, 3 or 4. The presence of unidirectional cross-bedding (indicative of hydrodynamic transportation: R.J.F. Jenkins, pers. comm.) and a very fine clastic component, suggests that these carbonates represent distal turbidites. This unit is 220 m thick at North Mount Goddard and 100 m thick at Black

Range Springs. At South Mount Goddard this unit is indistinguishable from the upper units of the Burr Well Member (see below), and therefore, is classed as part of that unit.

2.4 Burr Well Member

The basal section of the South Mount Goddard section is characterized by the absence of Units 1 and 2 and most of Unit 3, and notable thinning of the underlying Bunyeroo Formation (Haines, 10987; DiBona, 1989). In its place is a sequence consisting of a micritic dolomite unit that superficially resembles the Wearing Dolomite, which is followed by intraformational conglomerates and calcareous shales that grade into a series of thick-bedded limestones and thinly-bedded, maroon shales. This sequence, termed the Burr Well Member (DiBona, 1989) is approximately 110 m thick and passes upward into the olive-green shales and limestones of undifferentiated Units 4-8.

2.5 Units 4-8

It is not possible to clearly separate these units in the study area, so they are grouped together here. This sequence is 540 m and 410 m thick at the North and South Mount Goddard sections, respectively, where it comprises predominantly flatly laminated, olive-green, calcareous shales interbedded with packets of thin to very thinly interbedded grey-green limestone and olive-green shale. The limestone and shale intervals are generally very rhythmically bedded, but distinct packages or cycles on a scale of one to a few meters (detectable by small variations in bed thickness or limestone/shale ratio changes) are present and are often enhanced by weathering (Plate 2.a and 2.b). Cupriferous horizons are common at the base of this sequence in the study area. The graded bedding apparent in some of the limestones suggests carbonate settling from suspension, possibly representing a distal turbidite "tail" (Haines, 1987). Two minor intraformational conglomerates, thought to represent storm induced reworking of partially lithified sediments, were found in the North Mount Goddard section.

Minor, fine grained sandstone turbidites and more proximal limestone turbidites (Plate 2.c) indicate the progressive shallowing of the unit upsection and increased storm activity. Roughly 15 m from the top of this unit occurs the slightly sandy Purple Marker

PLATE 2

2.a Units 4-8 as seen at South Mount Goddard, showing the distinct limestone and shale packages, which are highlighted by weathering.

2.b Fine-grained limestone turbidite bed characteristic of the upper part of Units 4-8. Parallel bedding (T_B) passes up into sets of climbing ripples (T_C). Two generations of climbing ripple formation are seen.

2.c Finely interbedded shale and limestone packages. Scour surfaces, load casts and water escape structures are seen. Hammer is 30 cm long.

where?

2.a

2.b

2.c

Horizon (Figure 6.1), characteristic of mid- to upper-Unit 8 (Haines, 1987).

In the Black Range Springs section a sequence more correlatable with Haines (1987) subdivisions is observed. It comprises a shallowing-upward sequence of mainly silty, but occasionally sandy, carbonates interbedded with calcareous shales. Sandy limestones occur in the upper part of the sequence (Unit 8 equivalent), where the characteristic, slightly sandy, Purple Marker bed occurs.

2.6 Unit 9

In the Mount Goddard Syncline a thick succession of hummocky cross-stratified calcareous sandstones is interpreted to represent the lateral equivalent of Unit 9, and possibly the upper part of Unit 8 (Haines, 1987). This unit is 100 m thick at South Mount Goddard. In the North Mount Goddard section this unit is 130 m thick and contains an erosional boundary a few metres above its base. This boundary is likely to be a sequence boundary, due to the fluvial character of the overlying sandstones.

In the Black Range Springs section the equivalent of Unit 9 is seen as a 43 m thick package of shallow water, sandy dolomites and limestones which show cross-bedding, ripple marks and wavy bedding. Approximately 18 m below the base of this unit (which is defined as the base of a trough cross-bedded sandy dolomite) occurs the fossil horizon of *Palaeopascichnius*.

2.7 Units 10 and 11

Equivalents of these units are difficult to discern in the Mount Goddard sections where the Unit 9 equivalent is overlain by a poorly exposed sequence in which only the sandstone lithologies crop out. At North Mount Goddard, scattered outcrops of massive to thickly bedded grey limestones are seen in the first 50-60 m of measured section, whereas no limestone outcrop was observed at South Mount Goddard. This limestone unit is overlain by a thick sequence of sandstone and quartzite termed the "Upper Sandstone Unit" (Scotford, 1984; DiBona, 1989) which is inferred to be the equivalent of the very top of Unit 11 (Haines, 1987). This unit is 150 m thick at South Mount Goddard and 285 m thick at North Mount Goddard.

At Black Range Springs the equivalent of Unit 10 is approximately 30 m thick and comprises reddish sandstone units interbedded with green shales and occasional rarer, thin, dolomite beds. Unit 11 is seen as a 100 m sequence of interbedded very sandy dolomite and limestones. Some units were found to be oolitic and/or peloidal upon thin-section analysis.

The thickening of this unit, from 100 m Black Range Spring, to 150 m at South Mount Goddard and 285 m at North Mount Goddard, reflects increased subsidence away from the diapiric high (Scotford, 1984).

2.8 Origin of the Wonoka Carbonate

The carbonate of the Wonoka Formation is interpreted to have precipitated directly from sea water as a carbonate mud into the shelf environment. This inorganic phenomenon, known as "whitings", has been reported to occur in some lakes (Strong and Eadie, 1978, cited in Haines, 1987) and in some warm shallow marine environments (Cloud, 1962; Shinn et al., 1985). The driving force for this process is the extraction of CO_2 by photosynthetic algae from surface waters saturated with respect to $CaCO_3$ (Brasier, 1991). This CO_2 "draw down" mechanism for whitings production has been previously suggested by Tucker (1983, 1986) as the origin of late Precambrian shelf carbonates in the Biri Formation, southern Norway, and in the Virgin Spring and Sour Dough Limestones of California. The same process has been invoked for the genesis of the Bahama Shelf carbonates (Shinn et al., 1989; Robbins and Blackwelder, 1992). Slow precipitation of carbonate as whitings directly into the shelf environment, which is also receiving fine siliciclastics in suspension, could explain the mixed composition of the Wonoka Formation and the lack of interbedded mudstone (Haines, 1987). This carbonate is thought to have been originally been aragonitic by previous authors (Haines, 1987; DiBona, 1989), an interpretation which is supported by high strontium values (around 2,500 ppm) found in the present study (Appendix 5).

2.9 Measured Sections and Sample Selection

Samples from two sections (North Mount Goddard and Black Range Springs: Figure 2.1) were analysed for carbon and oxygen isotopes. Material from South Mount Goddard

was not selected for isotopic analysis due to the incomplete outcrop and lack of carbonate units in the upper part of the section. Sample locations along each section are shown on Figure 2.1.

Twelve samples form the North Mount Goddard section, and sixteen from the Black Range Springs section, were chosen for isotopic analysis using the following criteria:

1) Homogeneity, with very homogeneous limestone samples being preferred.

2) Carbonate content. This was determined by loss on ignition (see Appendix 5). Samples with less than 10% carbonate were not considered suitable for isotopic analysis.

3) Visible affects of alteration. Highly fractured and veined limestones and/or samples that showed obvious recrystallization were avoided.

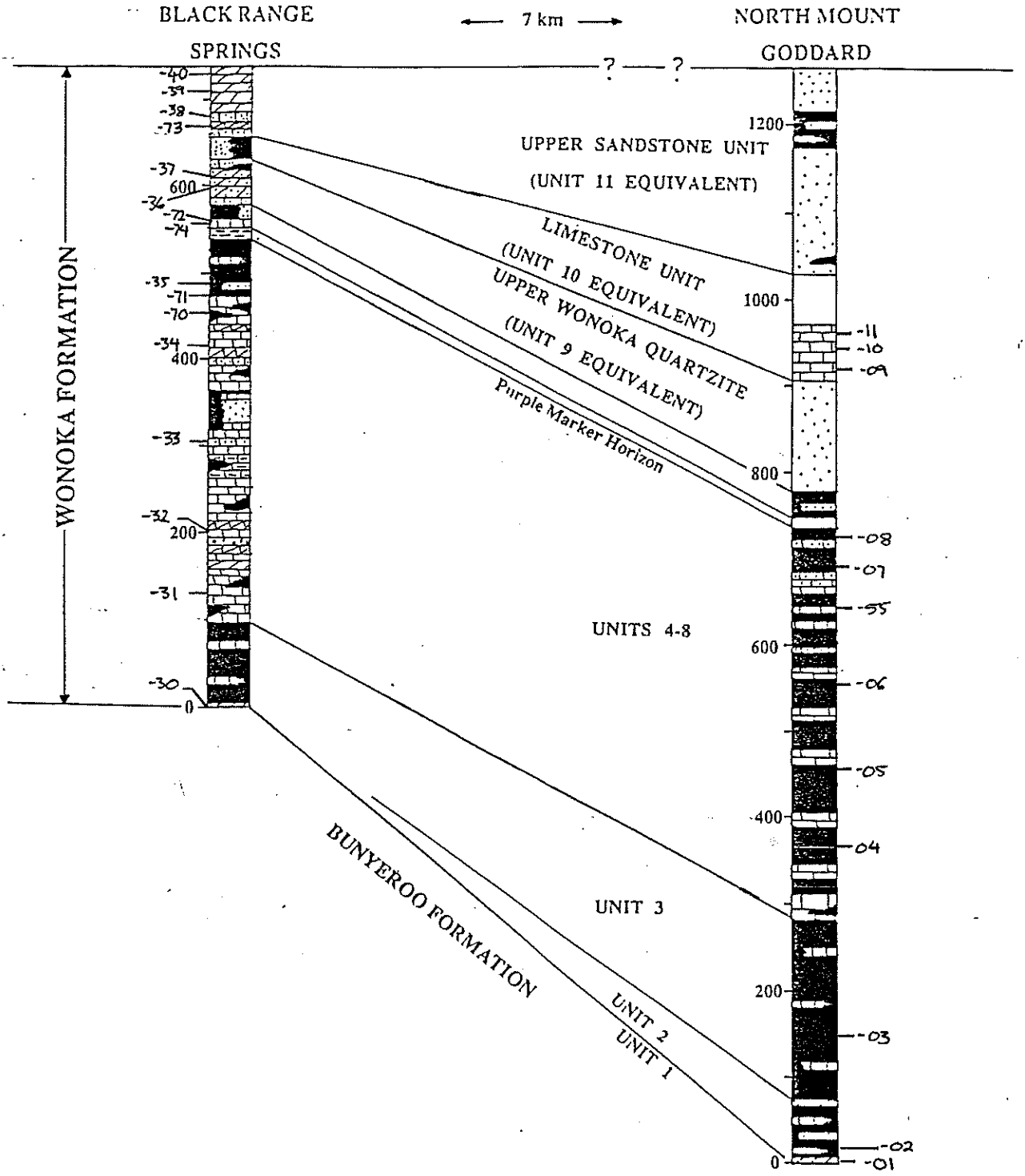

Figure 2.1 Positions of samples geochemically analysed along the Black Range Springs and North Mount Goddard sections..

CHAPTER 3 ANALYTICAL PROCEDURE

3.1 Geochemical Analysis

Representative portions of the twenty-eight samples selected for geochemical analysis were crushed and milled to a very fine powder using a tungsten-carbide mill. This powder was then used for total carbonate determination, X-ray diffraction and atomic absorbtion spectroscopy.

Total Carbonate Determination

Approximately 3-4 g of powdered sample was dried for a minimum of 4 hours at 110°C oven. An aliquot of dried powder was weighed into a clean alumina crucible, placed in a furnace at 500° for one hour, allowed to cool, weighed again, and heated 1000°C for one hour before being weighed a final time. The percentage weight losses after roasting at 500° and 1000°C are considered to be the organic and carbonate carbon contents of the sample, respectively. Unfortunately comparison with data obtained by Pell (1989) and Jansyn (1990) showed that the estimation of organic carbon content using this procedure is not accurate.

X-Ray Diffraction

A small amount of powdered sample was mixed with 3-4 drops of deionized water and spread evenly over a thin section slide. This was then dried in a 110°C oven and slide analysed in a Siemens X-Ray Diffractometer. The calcite:dolomite ratio of each sample was determined using the method of Tennet and Berger (1957).

Atomic Absorbtion Spectroscopy

One gram of sample was reacted overnight with 20 ml of 5 N acetic acid to preferentially dissolve out the carbonate fraction of the rock, then evaporated to dryness. A further 10 ml of 5 N acetic acid was then added and the non-carbonate residue was filtered out using a Whatman 52 hardened filter paper. Each solution was made up to 100 ml, with 10 mls of La/K solution (2% wt in 0.5 M HCl). Samples were analysed for elements Fe,

Mn, Sr, Mg, Ca and Rb on the Varian AA-6 Atomic Absorption Spectrometer using an air/acetylene flame and appropriate cathode lamp. The parts per million values were calculated using the Multi-Element Program for AAS Analysis and corrected to give the concentrations for the carbonate portion of the sample.

Carbon and Oxygen Isotopes

Representative aliquots of the individual samples, were removed from hand specimens with a drill, taking care to avoid weathering and veining. This powder was then analysed for the following isotopic ratios.

The twenty-eight samples screened in the above procedures were analysed for their whole rock $\partial^{13}C$ and $\partial^{18}O$ signatures. Samples that contained both dolomite and calcite were analysed separately to determine the isotopic composition of both carbonate phases. All values are reported in delta (∂) notation relative to the PDB standard and were automatically corrected for ^{14}C and ^{17}O by the computer. The formula used to calculate ∂ values is given as:

$$\partial^{13}C = \frac{(^{13}C/^{12}C_{sample} - {}^{13}C/^{12}C_{standard})}{(^{13}C/^{12}C_{standard})} \times 1000$$

(substitute ^{18}O, ^{16}O for ^{13}C, ^{12}C respectively for determination of $\partial^{18}O$)

Strontium Isotope Determination

Five samples were selected for strontium isotope analysis, based on criteria outlined by Kaufman et al. (1992), Derry et al. (1989, 1991) and Asmerom et al. (1991). The complex sample preparation procedures applied for strontium isotope analysis will not be discussed here. Analysis was performed manually on the Finnigan MAT261 Mass Spectrometer to obtain the $^{87}Sr/^{86}Sr$ isotopic ratio of each sample.

3.2 Petrographic Analysis

In an effort to determine the general petrographic composition of the samples

collected for isotopic analysis and to assess the extent of their diagenetic alteration (i.e. recrystallization and cementation) both cathodoluminescence (CL) and normal light microscopy techniques were employed. However, due to the micritic nature of some samples these techniques could not always be applied. In such cases, XRD analysis was used to determine mineralogy, and major and trace element analyses only were used to assess the extent of alteration.

One side of all thin-sections was stained using a mixture of Alizarin Red and potassium ferricyanide (Dickson, 1965). Staining of samples is essential for determining calcite chemistry (i.e. separating magnesian calcite from ferroan calcite) which, in turn, is vital in elucidating cementation and for highlighting calcite crystal morphologies which are otherwise indistinguishable.

CHAPTER 4 STABLE ISOTOPE COMPOSITION

Results of stable isotopic analysis of the selected samples are presented in Table 4.1. All values are reported in parts per mil (‰), relative to the PDB standard. These values have been plotted against stratigraphic height in Figures 4.1.a and 4.1.b.

4.1 Oxygen Isotope Signature

A very homogeneous oxygen isotopic signal is seen for the greater part of each section, with excursions to less negative values apparent in the lower and upper portions of the sections. North Mount Goddard shows the largest variation in oxygen isotopic signal, with $\partial^{18}O$ values ranging from -8.4 to -15.9 ‰. Values obtained from the Black Range Springs, -9.3 to -14.8 ‰, show a much more uniform signal upsection.

The primary $\partial^{18}O$ signature of any marine limestone is dependent on two factors, the isotopic composition of the seawater, and the temperature at which the carbonate was precipitated. A third factor, termed vital effect, may be associated with biogenic carbonates, but does not apply here. Due to the susceptibility of oxygen isotopes to alteration during diagenesis (Magaritz, 1983; Veizer, 1983; Marshall, 1991), the observed values are considered more likely to represent the isotopic composition and temperature of the diagenetic porefluids present during burial diagenesis and/or metamorphism, rather than the primary signal of the depositing sea water. An involvement of ^{18}O-depleted meteoric waters could be advocated as an alternative, or complementary, cause of isotopically light shallow-water carbonates.

Temperatures reached during burial and metamorphism of the Wonoka Formation have been estimated to be approximately 165-180°C (D. M. McKirdy, pers. comm.). Recrystallization at elevated temperatures leads to a depletion of ^{18}O (and therefore a decrease in the $\partial^{18}O$ values) in the precipitating carbonate phase (Tucker and Wright, 1990). This is evident in the homogeneity of the $\partial^{18}O$ signature seen at the Black Range Springs section, and for the lower portion of the North Goddard section (Fig. 4.1.a and 4.1.b). These $\partial^{18}O$ values are thus interpreted to be the result of thermal homogenization at elevated temperatures, and therefore are of little stratigraphic use. The excursion to heavier

isotopic values at the top of the North Mount Goddard section is thought to be a reflection of interaction with isotopically negative pore-fluids during burial diagnesis and/or metamorphism.

North Mount Goddard				Black Range Springs			
Sample No.	Meterage	$\partial^{13}C$	$\partial^{18}O$	Sample No.	Meterage	$\partial^{13}C$	$\partial^{18}O$
977-01	0	-0.1	-9.3	977-30	0	-1.7	-9.3
977-02	10	-6.4	-14.9	977-31	130	-7.5	-14.9
977-03	145	-9.0	-15.9	977-32	202	-6.3	-14.2
977-04	375	-7.5	-15.0	977-33	300	-6.9	-14.1
977-05	465	-6.4	-14.7	977-34	416	-6.1	-14.7
977-06	545	-6.0	-13.4	977-70	448	-6.3	-13.4
977-06	630	-5.2	-14.7	977-71	467	-4.9	-14.7
977-07	680	-4.8	-14.3	977-35	483	-3.9	-13.4
977-08	730	-1.2	-15.1	977-74	534	-1.9	-14.1
977-09	946	-3.3	-9.8	977-72	576	4.7	-14.3
977-10	965	1.7	-10.1	977-36	600	2.9	-13.6
977-11	985	-1.1	-8.4	977-37	623	4.5	-13.2
				977-73	684	3.4	-12.4
				977-38	689	3.5	-12.0
				977-39	739	6.6	-11.9
				977-40	754	6.5	-11.5

Table 4.1 Summary of isotopic analysis of selected samples for North Mount Goddard and Black Range Springs sections. Meterages refer to height above datum.

4.2 Carbon Isotopic Signature

Each section begins with a relatively low negative $\partial^{13}C$ value for the basal, Wearing dolomite, -0.08 ‰ at North Mount Goddard and -1.7 ‰ at Black Range Springs, which is considered to be a reflection of the unit's shallow-water origin. This is followed by a sharp negative excursion to values of -8 to -9 ‰ in Unit 3. Thereafter the carbon isotopic signal of the Wonoka Formation shows a progressive trend towards more positive values upsection (Figure 4.1.a and 4.1.b).

At Black Range Springs this signal varies from -7.6 to -6.1 ‰, remaining relatively constant for over a thickness of 460 m, before showing a progressive excursion to more positive values. This excursion begins at a stratigraphic height which corresponds approximately with the Unit 7/8 transition and increases consistently to a value of +4.7 ‰. Two negative pulses are seen before a maximum value of +6.6 ‰ is reached near the top of the formation.

The isotopic trend seen at North Mount Goddard is very similar. Beginning with a relatively consistent negative signal which varies from -8.9 to -6.0 ‰, and continues for a vertical stratigraphic interval of approximately 600 m. The signal observed here for the lower portion of the Wonoka Formation differs slightly from that seen at Black Range Springs in that, although it is still very negative, it shows steady shift towards positive values. A marked shift to more positive values occurs at a stratigraphic height equivalent to that of a similar shift in the Black Range Springs profile, namely, at the Unit 7/8 boundary. Due to the lack of any substantial carbonate units in the upper Wonoka Formation at North Mount Goddard, detailed analysis was not possible. The three samples analysed from the limestone unit present show a positive excursion from -3.3, to +1.7 ‰, before returning to -1.1 ‰ (see Figures 4.1.a and 4.1.b), suggesting that similar oscillations are preserved in the isotopic record of the upper Wonoka Formation in both sections.

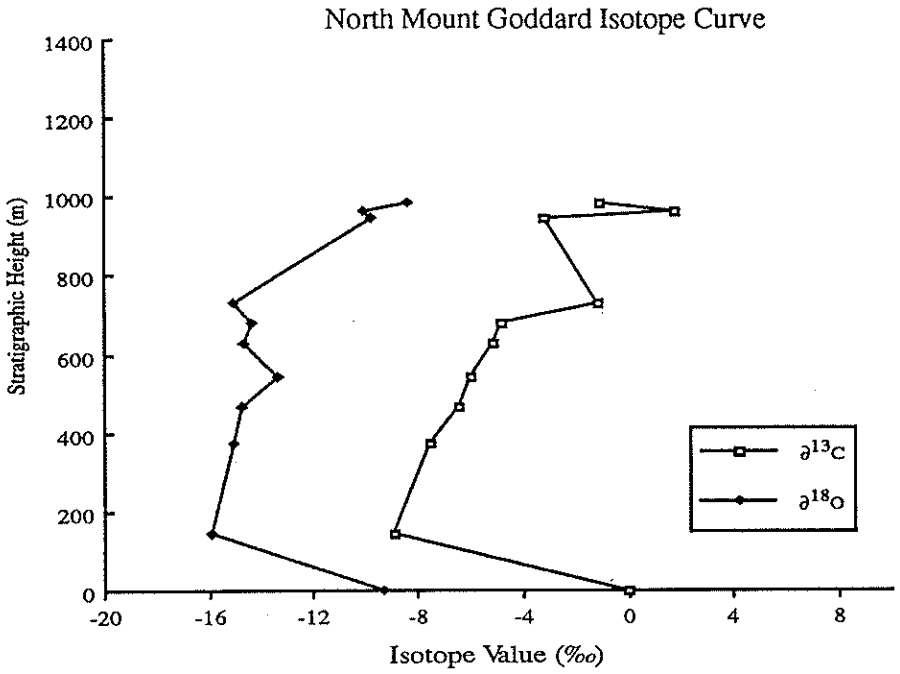

Figure 4.1.a Isotope curves for Black Range Springs section. Total thickness of Wonoka Formation is 760 m.

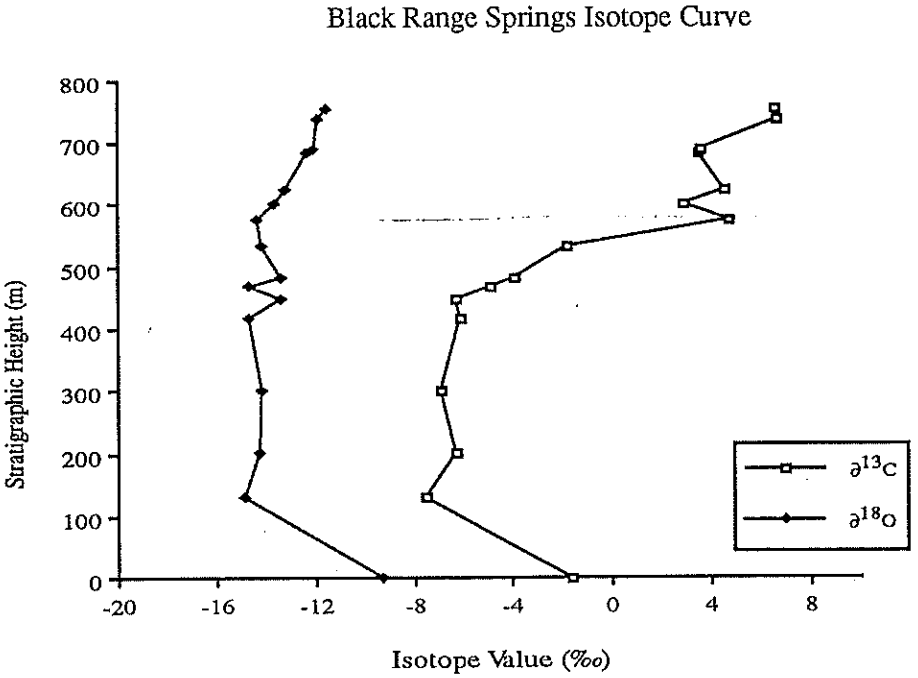

Figure 4.1.b Isotope curves for North Mount Goddard section. Total thickness of Wonoka Formation is 1310 m.

CHAPTER 5 DIAGENESIS OF LIMESTONES

5.1 Diagenetic Processes

5.1.1 Dolomitization

Many of the samples selected for carbon and oxygen isotopic analysis have been partially dolomitized. The $\partial^{13}C$ signature of these and other late Proterozoic carbonates has been shown to be little affected by this process, since the bulk of the carbon atoms are derived from the original carbonate phase (Derry et al., 1992; Table 5.1). However, the oxygen isotopes have been found to fractionate by approximately 3 ‰ (Tucker and Wright, 1990; Veizer et al., 1992). This is evident in the separate analysis of calcite and dolomite portions of partially dolomitized samples of the Wonoka Formation (Table 5.1). The fractionation of the oxygen isotopes observed in this study falls within the range suggested by Land (1980) for a cogenetic mineral pair.

Sample No.	$\partial^{13}C$ Calcite	$\partial^{13}C$ Dol.	$\Delta^{13}C$ (Calc-Dol)	$\partial^{18}O$ Calcite	$\partial^{18}O$ Dol.	$\Delta^{18}O$ (Calc-Dol)
North Mount Goddard						
977-07	-4.81	-4.85	0.04	-14.34	-10.82	-3.52
977-08	-1.18	-1.81	0.63	-15.06	-11.66	-3.40
Black Range Springs						
977-31	-7.55	-6.90	-0.65	-14.88	-13.52	-1.36
977-32	-6.30	-5.88	-0.42	-14.20	-12.85	-2.71
977-34	-6.14	-5.10	-1.04	-14.66	-6.93	-7.73
977-70	-6.30	-5.84	-0.46	-13.36	-10.08	-3.28
977-71	-4.91	-5.19	0.28	-14.65	-11.35	-3.30
977-35	-3.94	-3.48	-0.46	-13.42	-10.46	-2.96
977-74	-1.86	-3.07	1.21	-14.13	-10.24	-3.89

Table 5.1 Summary of isotopic analysis of separate carbonate phases, showing magnitude of fractionations for each phase.

5.1.3 Metamorphism

The elevated temperatures characteristic of deep burial and metamorphism have been shown to deplete ^{18}O in the carbonate by approximately 10 ‰ for every 100°C rise in temperature (Brasier et al., 1992; Hudson, 1977). Smaller effects are to be expected for the carbon isotope composition, due to its non-dependence upon temperature. The $\partial^{13}C$ values in the carbonates of the Wonoka Formation show wide variation, and still retain distinct trends, unlike the relatively constant and apparently homogenised $\partial^{18}O$ values (Fig.4.1.a and 4.1.b, Chapter 4). The dewatering of clays during progressive metamorphism will also strongly affect the $\partial^{18}O$ signature (N.M. Lemon, pers. comm.).

5.1.4 Bacterial Decay of Organic Matter

Enrichment of ^{12}C in carbonate cements may occur where there is incorporation of biogenic CO_2 from the bacterial decay of organic matter in organic-rich sediments (Irwin et al., 1977). However, the Wonoka Formation is organically very lean (TOC values consistently less than 0.05 wt%: Pell, 1989; Jansyn, 1990), a feature common to carbonates from both reducing and oxidising settings. Therefore, such biogenic CO_2 is likely to have had little or no effect on the isotopic composition of the Wonoka Formation during early diagenesis.

5.1.5 Thermal Alteration of Organic Matter

This process is unlikely to have affected the carbon isotopic signal of the Wonoka Formation. As stated previously, the Wonoka Formation has a very low organic carbon content, and its incipient metamorphism in the study area (lower greenschist facies, chlorite zone: McKirdy et al., 1975) is unlikely to have produced significant amounts of ^{13}C-depleted CO_2. This is supported by analysis of maturation levels of kerogen in the study area (H/C atomic ratios of 0.46 to 0.54: N.M. Lemon, pers. comm.). Significant shifts to heavier kerogen $\partial^{13}C$ values occur only at much higher maturation levels (H/C <0.2: D.M. McKirdy, pers. comm.), showing that there has been minimal isotopic adjustment due to residual organic matter.

5.2 ASSESSMENT OF DIAGENETIC ALTERATION

To assess the extent to which ancient carbonates have been altered, and therefore retain their carbon isotopic signature, previous authors have adopted several geochemical strategies. Some of these methods have been applied in the present study and are outlined below.

5.2.1 Trace and Major Element Ratios

Measurement of concentrations of diagenetic tracers, such as Mn, Fe, Sr, Mg and $^{87}Sr/^{86}Sr$, allows an independent assessment of the degree of diagenetic alteration (Veizer, 1983; Fairchild et al., 1990; Marshall, 1991). In the present study the concentrations of Mg, Ca, Sr and Mn were utilized for this assessment. A summary of the pertinent analytical data is presented in Table 5.2.

Mg will only show a diagenetic depletion if the original phase was high magnesium calcite (HMC: Magaritz, 1983; Veizer, 1983; Marshall, 1991). Mg concentrations in pure carbonates in the Wonoka Formation are low (approximately 4000-8000 ppm in samples with no dolomite component); higher Mg concentrations are only seen in samples that contain dolomite (Table 5.2). This is consistent with the mineralogical stabilization of the original aragonite phase (Singh, 1986; Haines, 1987; DiBona, 1989) to diagenetic low magnesium calcite (dLMC).

Sr and Mn are excellent indicators of alteration because of their widely divergent partition coefficients (fractionation factors), their association mainly with the carbonate lattice, and their vastly different abundances in marine and meteoric water (Brand and Veizer, 1980). Samples considered to have seen the fewest dissolution/reprecipitation events (and/or the least amount of diagenetic fluid flow) have the highest Sr, and lowest Mn concentrations. The inverse relationship between these two elements can be seen in Figure 5.1, where the trend towards increasing alteration (or, alternatively, an open diagenetic system) is to the right.

The ratio of these two elements provides the best estimate of alteration for individual samples. Samples with high Mn/Sr concentrations (>3) are considered to be the product of a relatively open diagenetic system, or "altered". The basal dolomite samples (A977-01 and

A977-30) were precluded from this analysis because their Mn/Sr ratios are elevated due to the lack of Sr in the dolomite lattice.

Sample No.	Meterage	Mg ppm	Ca ppm	% Dol.	Mn ppm	Sr ppm	Mn/Sr
North Mount Goddard							
977-01	0	102443	234849	95	7206.8	149	48.45
977-03	145	4132	437450	0	3454.4	231	14.70
977-04	375	4182	470583	0	1247.5	1138	1.10
977-05	465	3782	424539	0	748.8	5228	0.14
977-06	545	3352	497853	0	678.0	2736	0.25
977-55	630	9919	455280	0	1082.6	1309	0.83
977-07	680	77670	421914	50	4091.5	517	7.92
977-08	730	37679	462890	33	2477.9	659	3.76
977-09	946	2972	365470	0	249.4	239	1.04
977-10	965	52323	119546	0	803.0	68	11.77
977-11	985	1307	419673	0	231.4	269	0.86
Black Range Springs							
977-30	0	35567	1013193	95	10448	92	5.74
977-31	130	18334	424393	18	1825.6	394	4.63
977-32	202	15780	413090	13	1653.2	1550	1.07
977-33	300	8852	457087	0	991.0	2794	0.36
977-34	416	18330	387870	14	1368.0	993	1.38
977-70	448	57467	343482	45	1562.0	351	4.45
977-71	467	29195	369612	30	915.4	582	1.57
977-35	483	24771	372695	23	2498.2	433	5.77
977-74	534	47593	342619	35	2456.9	343	7.16
977-72	576	4005	453592	0	2767.0	567	4.88
977-36	600	4537	466130	0	2027.4	621	3.26
977-37	623	3857	500267	0	892.3	381	2.34
977-73	684	15552	440373	5	730.1	280	2.81
977-38	689	5984	466164	0	190.1	172	1.10
977-39	739	7624	462526	0	373.1	203	1.84
977-40	754	8073	459434	0	386.8	208	1.86

Table 5.2 Summary of trace and major element analysis of samples for North Mount Goddard and Black Range Springs sections.

Mn/Sr ratios have been plotted against $\partial^{13}C$ values in Figures 5.2.a and 5.2.b. No correlation is apparent between these two parameters, indicating that there is no relationship

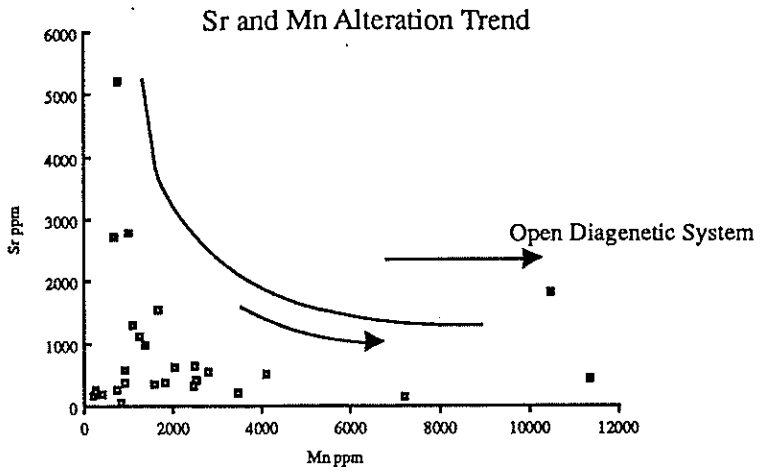

Figure 5.1 Cross-plot of Sr and Mn, showing geochemical trend with increasing alteration

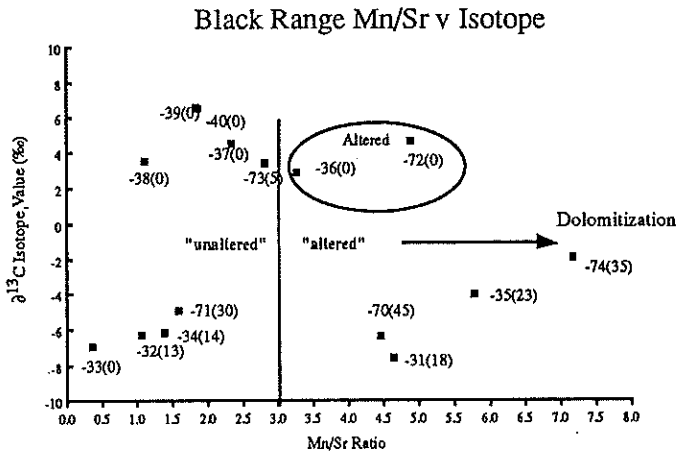

Figure 5.2.a Carbon isotope values plotted against Mn/Sr ratios, showing no relationship between the two variables. Figures in brackets refer to the dolomite content of each sample.

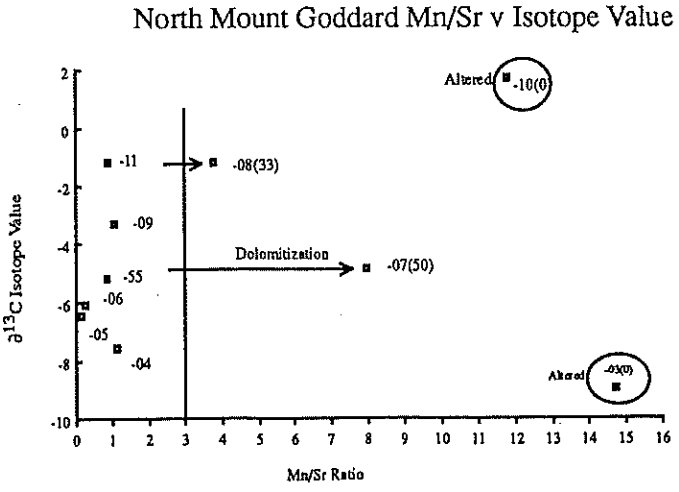

Figure 5.2.b Carbon isotope value plotted against Mn/Sr ratios, no correlation is apparent. Values in brackets refer to dolomite content of samples. Points with no bracketed value have no dolomite content.

between "alteration" and isotope value according to this method of assessment. This suggests that the alteration of these samples has not been severe enough to significantly alter the carbon isotopic values.

Those samples with a ratio of <3 have undergone the least diagenetic alteration, and were therefore considered to retain unaltered isotopic signatures. However, some samples contain dolomite. Dolomitization does not significantly alter the $\partial^{13}C$ values of samples (Table 5.1, section 5.1.1) but it does substantially raise Mn/Sr ratios. Values in brackets refer to the percentage dolomite in individual samples. Calcite and dolomite phases were not analysed separately for major and trace element concentrations, and therefore the Mn/Sr ratios of these samples will reflect not only the degree alteration of the calcite phase, but also the degree of dolomitization. For this reason samples A977-70, and -08 are classified here as unaltered, even though they plot in the altered field. Samples A977-36, -72, -10 and -03 are classified as altered because they have high Mn/Sr ratios (>3) and no dolomite component. Samples A977-31, -74, -35 and -07 cannot be classified as either altered or unaltered using this method of assessment. All of these samples have high Mn/Sr ratios (ranging from 4.5 to 8) but also are relatively highly dolomitized (from 23 to 50 %). Separate geochemical analysis of the two carbonate phases is required to accurately assess the alteration of these particular samples.

5.2.2 $\partial^{13}C$ and $\partial^{18}O$ Covariation

Covariation between $\partial^{18}O$ and $\partial^{13}C$ also has been used as a diagenetic marker (Kaufman et al., 1992). A positive correlation between these two variables is thought to be indicative of alteration via the result of the mixing of fluids with different isotopic composition, namely meteoric water and sea water (Kaufman et al., 1992). More negative values of both $\partial^{18}O$ and $\partial^{13}C$ are produced by a higher meteoric input (Tucker and Wright, 1990). A weak covariance is seen in the present study (Fig. 5.3a+5.3b) however, due to the possible thermal homogenization of the $\partial^{18}O$ signature of some samples during metamorphism this indicator of alteration was considered not to be directly applicable. Where used, this method has been shown to be unreliable in detecting alteration in many cases. A single cementation event may lead to covariance of the isotope signatures, but

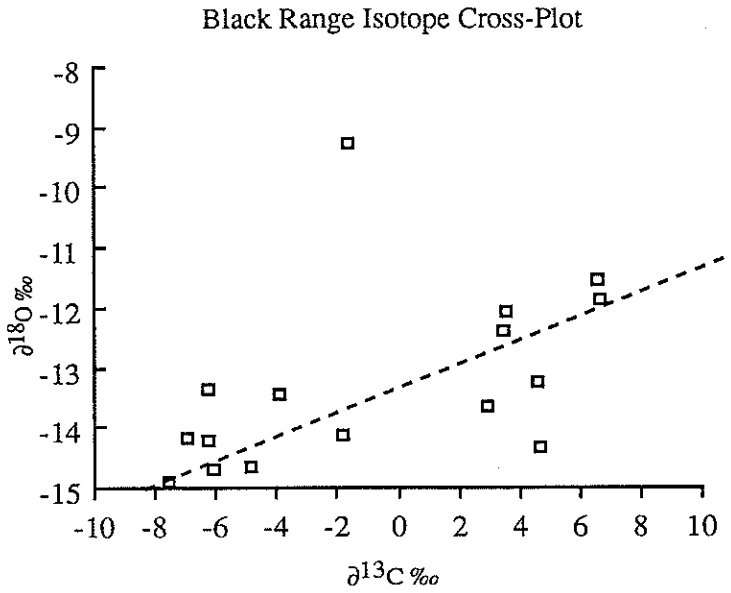

Figure 5.3.a Isotopic cross-plot for Black Range Springs section.

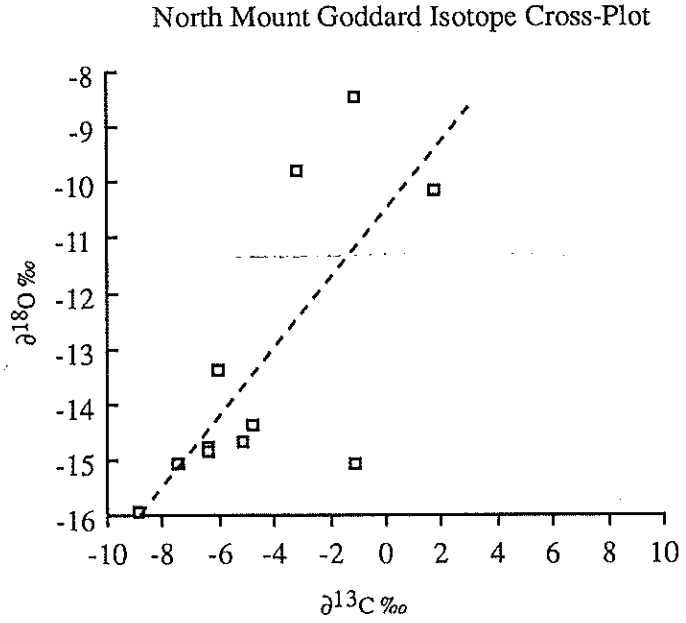

Figure 5.3.b Isotopic cross-plot for North Mount Goddard section.

where varying mixtures of meteoric and sea water (and/or changes in temperature during crystallization) are involved, more complex, non-linear patterns may emerge (Marshall, 1991).

5.2.3 Petrographic Analysis

Petrographic assessment of the carbonates of the Wonoka Formation involved the use of both conventional light microscopy and cathodoluminescence (CL). For detailed thin-section and petrographic descriptions see Appendix 1. Classification of samples (using Folk's classification scheme) and the analysis of grain size, cementation phases and cement chemistry, has revealed two major groups of samples.

The first group comprises the deep-water, thinly bedded limestones, interbedded with shales. Samples of this group are generally micritic to microsparitic, show signs of minor mechanical compaction (bedding plane orientated muscovite and opaques: Tucker and Wright, 1990) and lack evidence of chemical compaction (i.e. stylolites). Euhedral quartz and albite crystals are common. Vugs filled with burial ferroan cement were found in samples A977-04, -06 and -34 (Plate 5.a). The varying amounts of ferroan burial cement in the samples of this group appear to have had little effect upon their $\partial^{13}C$ values (Table 5.3). The low porosity and resistance to fluid flow of these limestones, evident by their micritic nature and association with thick sequences of shales, is favourable for the retention of primary $\partial^{13}C$ signatures (Burdett et al., 1990; Knoll and Swett, 1990; Kaufman et al., 1991; Derry et al., 1992).

The second group is composed of the shallow-water, lagoonal limestones characteristic of the upper Wonoka Formation. Samples A977-10 (North Mount Goddard) and A977-72 (Black Range Springs) are the two samples considered to be altered in this group. Both show evidence of extensive recrystallization by various pore-fluids (Plate 5.b) . Although sample A977-37 shows evidence of pre-compactional lithification, this sample also exhibits five generations of cement (Plate 5.1.c), ranging from shallow burial diagenetic to meteoric. Due to the uncertain timing of these cementation phases, this sample cannot be regarded as having a primary isotopic signal. Isotopic and geochemical analysis of each cement phase is required to ascertain whether the whole-rock isotopic value obtained

PLATE 5

5.a Vug present in thin, distal limestone turbidites of the lower Wonoka Formation. Highly luminescent, ferroan burial cement fills original void, with authigenic quartz and/or albite surrounding the rim.

5.b Sample A977-72, showing recrystallization under the influence of varying pore-fluid chemistry.

5.c Sample A977-37, showing many cementation periods and different carbonate chemistries. Cemented intraclasts and grapestones are surrounded by a void filling, highly luminescent isopachous cement (Mg calcite) which is followed by a pore-occluding, dull-luminescent ferroan cement.

5.d Highly fractured and veined shallow-water limestone of the upper Wonoka Formation at Black Range Springs.

5.a

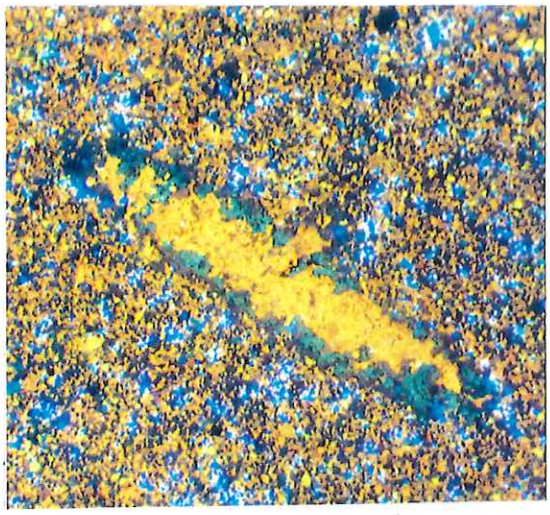

200um

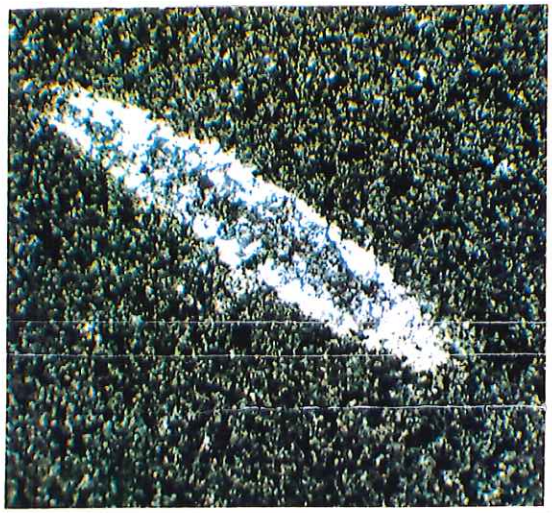

5.b

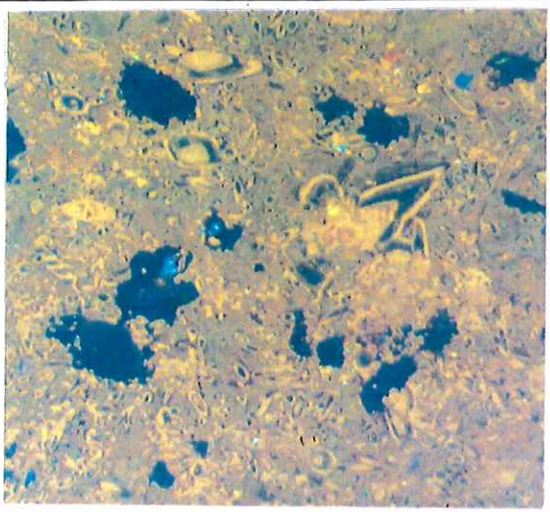

100um

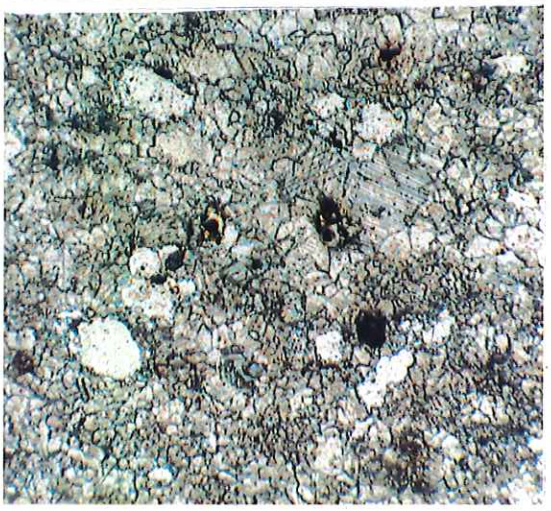

5.c

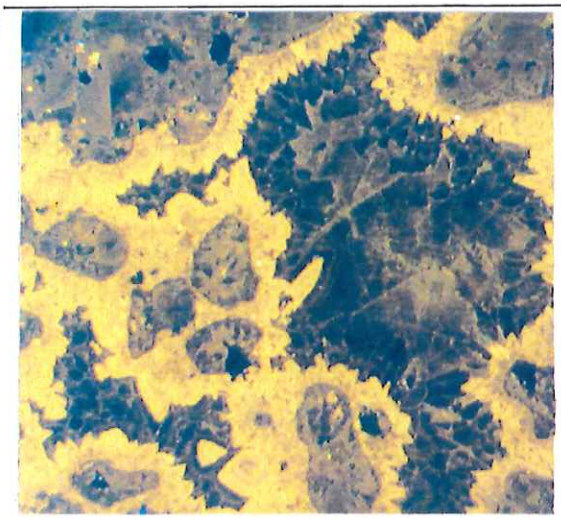

100um

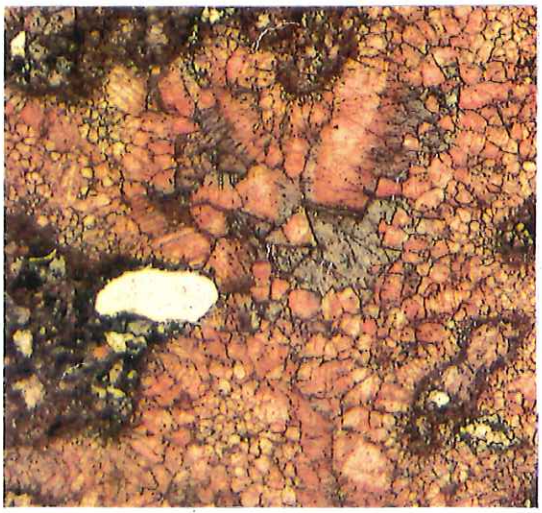

5.d

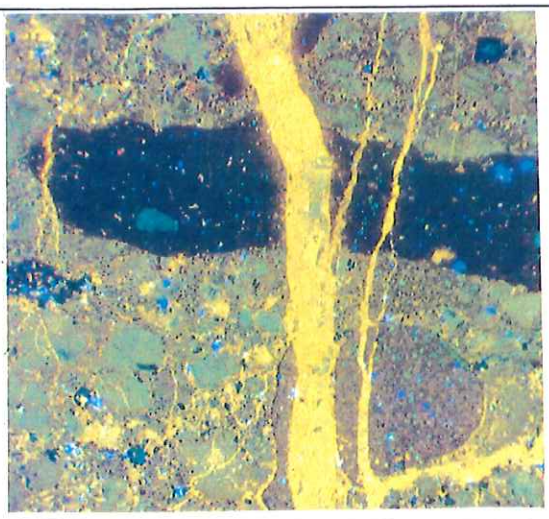

200um

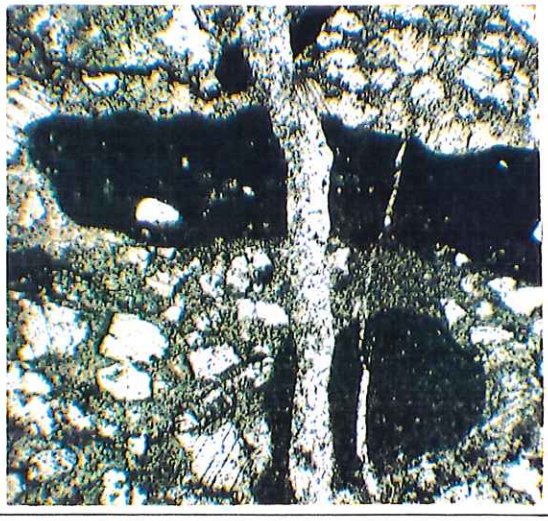

in the present study is an adequate measure of the depositing seawater chemistry. Sample A977-39 (a pel- to oo-sparite: see Appendix 1) shows major fracture-filling calcite veins (Plate 5.d), but this is considered unlikely to substantially alter the carbon isotopic value of such a relatively pure carbonate (86 % carbonate) (see Baker at al., 1982; Marshall, 1991)

Sample No	Burial Cement	Veining	Carbonate	% Carb	∂ 13C	Mn/Sr
North Mount Goddard						
Group 1						
977-01	None	Moderate	Microspar	83	-0.1	48.5
977-03	None	None	Microspar	62	-8.9	14.7
977-04	>90%	Minor	Microspar	70	-7.5	1.1
977-05	All	Minor	Microspar	65	-6.4	0.1
977-06	50%	Moderate	Microspar	53	-6.1	0.2
977-55	30%	None	Microspar	83	-5.1	0.8
977-07	All	None	Micrite	29	-4.8	7.9
977-08	80%	V. Minor	Micrite	51	-1.2	3.8
Group 2						
977-09	None	None	Microspar	40	-3.25	1.0
977-10	None	None	Sparite	40	1.7	11.8
977-11	None	None	Microspar	80	-1.1	0.9
Black Range Springs						
Group 1						
977-30	None	None	Microspar	20	-1.7	5.7
977-31	50%	None	Microspar	52	-7.6	4.6
977-32	All	None	Spar	51	-6.3	1.1
977-33	None	None	Microspar	62	-6.9	0.4
977-34	All	None	Micrite	37	-6.1	1.4
977-70	All	None	Micrite	38	-6.3	4.5
977-71	None	None	Microspar	54	-4.9	1.6
977-35	All	None	Micrite	29	-3.9	5.8
Group 2						
977-74	50%	None	Microspar	50	-1.9	7.2
977-72	30%	None	Spar	82	4.7	4.9
977-36	50%	None	Microspar	62	2.9	3.3
977-37	10-15%	Minor	Intraspar	86	4.5	2.3
977-73	None	None	Microspar	59	3.4	2.8
977-38	None	None	Spar	89	3.5	1.1
977-39	None	Major	Pel/Oospar	86	6.6	1.8
977-40	None	None	Intraspar	85	6.5	1.9

Table 5.3 Summary of sample groupings determined through petrographic analysis and compared with geochemical and isotopic values.

Samples A977-70, -31, -35 and -74, which could not be defined as altered or unaltered through geochemical analysis, are here classed as unaltered due to the lack of visible diagenetic alteration and the homogeneity of samples in thin-section. These samples fit the general isotopic trend (Fig. 4.1.a and 4.1.b), showing that they have not experienced significant alteration (Table 5.3).

5.2.4 Summary of Least Altered Samples

Table 5.4 summarizes the samples which have been classed as "least altered" on the basis of the aformentioned diagenetic assessment procedures. These samples are plotted against stratigraphic height in Figures 5.4.a and 5.4.b. Samples A977-03 and -10 (North Mount Goddard) and A977-36, -37 and -72 (Black Range Springs) are classified as altered and hence are not used to constrain the isotopic curves.

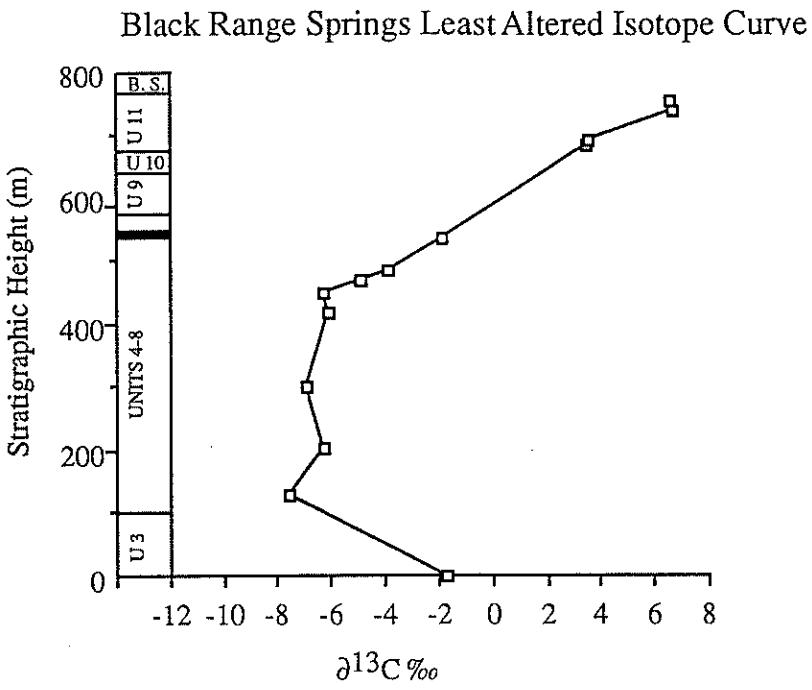

Figure 5.4.a Isotope curve for least altered samples from Black Range Springs section, showing the consistent trend to more positive values in Units 8 to 11.

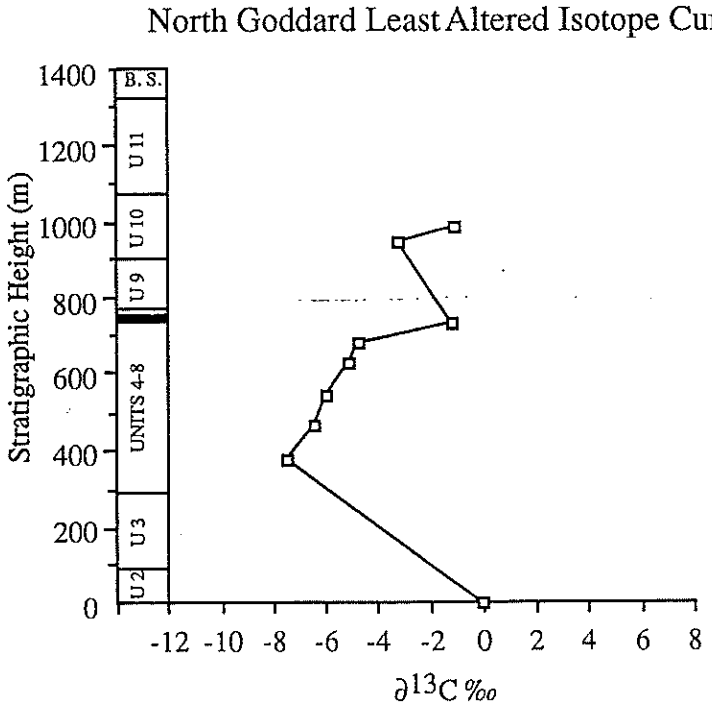

Figure 5.4.b Isotope curve of least altered samples for the North Mount Goddard section, showing a somewhat different positive trend upsection.

North Mount Goddard					
Sample No	Meterage	Mn/Sr	% Yield	% Dol.	$\partial^{13}C$
977-01	0	48.450	82.70	95	-0.08
977-04	375	1.096	70.30	0	-7.54
977-05	465	0.143	65.04	0	-6.43
977-06	545	0.248	53.10	0	-6.04
977-55	630	0.827	82.67	0	-5.16
977-07	680	7.920	28.84	50	-4.81
977-08	730	3.760	50.85	33	-1.18
977-09	946	1.040	39.70	0	-3.25
977-11	985	0.860	79.50	0	-1.13
Black Range Springs					
977-30	0	5.740	18.95	95	-1.69
977-31	130	4.630	51.49	18	-7.55
977-32	202	1.066	50.57	13	-6.30
977-33	300	0.355	62.36	0	-6.94
977-34	416	1.378	36.77	14	-6.14
977-70	448	4.450	37.90	45	-6.30
977-71	467	1.574	53.64	30	-4.91
977-35	483	5.770	28.42	23	-3.94
977-74	534	7.160	50.47	35	-1.86
977-73	684	2.810	58.90	5	3.44
977-38	689	1.100	88.90	0	3.54
977-39	739	1.840	86.30	0	6.61
977-40	754	1.860	84.80	0	6.54

Table 5.4 Summary of least altered samples, their meterage, dolomite content, diagenetic tracer value and isotope value.

CHAPTER 6 Correlation and Interpretation of the Wonoka Formation Carbon Isotope Signature

Any interpretation of the carbon isotope signature of late Proterozoic carbonates encounters certain problems, namely the isotopic overprints associated with secondary, post-depositional alteration. In the previous chapter an attempt was made to identify those samples that have undergone significant alteration. This chapter will attempt to interpret and explain the isotopic signature that appears to be characteristic of the Wonoka Formation. To do this, data from previous and concurrent investigations, namely, studies by Eickoff et al. (1988), Jansyn (1990) and Ayliffe (1992), must be called upon for comparison. Figure 6.1 provides a cross-basinal correlation of isotopic curves obtained from this and other studies of the Wonoka Formation at various localities.

The isotopic curves of the Wonoka Formation show a marked consistency across the Adelaide Fold Belt, as evident in Figure 6.1. For the purpose of interpretation and discussion, this isotopic curve may be separated into two parts. The first, termed the Lower Wonoka Signal, is the isotopically negative signal recorded in the lower two-thirds of the Wonoka Formation. The second part is characterized by a marked positive excursion, and is termed the Upper Wonoka Signal. The transition between these two isotopically distinct sections occurs at a lithologically consistent height, namely the Unit 7/8 boundary (or its equivalent at the present study location), just below to the purple marker horizon (Figure 6.1).

Location	Study	Mean Value	Range	Wall Plaster	I/C Clast	I/C Matrix
North Goddard		-7.24	-6.04 to -8.96			
Black Range	This Study	-6.65	-6.14 to -7.55			
Bunyeroo Gorge	Jansyn (1990)	-7.72	-7.41 to -8.61			
Pichi Richi	Ayliffe (1992)	-7.69	-7.35 to -8.02	-8.89	-8.3	-8.9
Fortress Hill	Eickoff et al (1988)			-8.86		

Table 6.1 Summary of present and previous investigations of the lower Wonoka Formation.

FIGURE 6.1 INTRA-BASINAL STRATIGRAPHIC AND ISOTOPIC CORRELATION OF THE LATE PROTEROZOIC WONOKA FORMATION

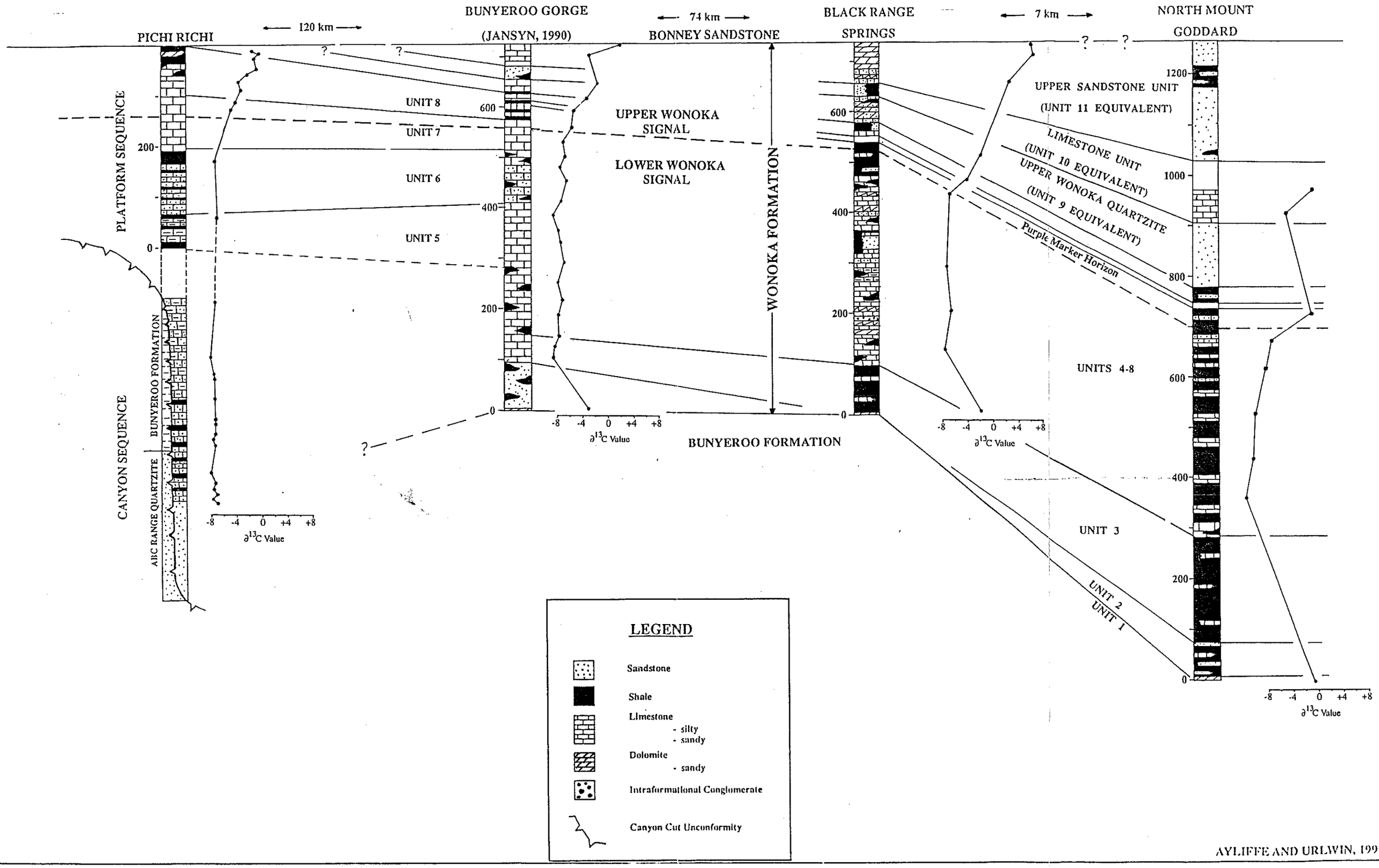

AYLIFFE AND URLWIN, 1992

6.1 Interpretation of the Lower Wonoka Signal

An important factor that needs to be considered when attempting to determine the origin of the very negative isotopic signature seen in the lower Wonoka Formation, is the signal's extreme consistency. Table 6.1 summarizes results obtained from this, and previous, studies of the lower Wonoka Formation, showing the narrow range and pervasiveness of this negative signal. Analysis of a clast (which has a high probability of retaining a primary isotopic signal: N.M. Lemon, pers. comm.) and matrix from an intraformational conglomerate, fracture filling-calcite veins (Ayliffe, 1992) and canyon associated wall plaster (Eickoff et al., 1988; Ayliffe, 1992) produced results consistent with the previously described negative signal (Table 6.1). Burial diagenetic and fracture-filling cements present in some samples are assumed to have derived their isotopic signal from the original carbonate phase. Such a pervasive signal is obviously not the product of localized primary or diagenetic influences, but must be the result of a basin-wide, isotopically uniform phenomenon. Any interpretation of this signal must satisfactorially explain this extreme consistency.

One possible interpretation is that this signal represents a primary isotopic signature, reflecting deposition and lithification in basinal waters that have an anomalously negative carbon isotopic signal. This extremely negative carbon signal is thought to be produced immediately after departure of the late Proterozoic climate from an ice-house state. A pulse of cold oxygen-rich bottom waters, produced by the retreat of the polar icecaps (Figure 6.2.b), ensures rapid bacterial oxidation of organic matter falling past the thermocline of a now stratified ocean. This stratification will prevent the resulting ^{12}C-enriched CO_2 from returning to the surface waters, thus rendering the bottom waters capable of producing "super-negative" carbonate. The glaciation invoked for this model is not associated with the Marinoan event (the last glaciation represented in sediments in the Adelaide Fold Belt), but is thought to be associated with a later Proterozoic glaciation, possibly occurring in the northern hemisphere. The effects of this glaciation are not represented in Adelaide Fold Belt sediments, but are inferred to be present. Depositional environments of the relevant Wonoka Formation units that contain this signal are shown in Figure 6.3.a and 6.3.b.

Isotope values of approximately -6 ‰ have been reported world wide for late

Precambrian carbonates (Brasier, 1991) and values as low as -10 ‰, interpreted to be primary, have been reported in Ohio (R.J.F. Jenkins, pers. comm.).

6.2 Interpretation of the Upper Wonoka Signal

The base of the Upper Wonoka Signal is defined as the start of the positive excursion seen in the general isotopic signature of the Wonoka formation. This shift occurs just prior to the purple marker bed, at a stratigraphic height of approximately 460 m at Black Range Springs and 600 m at North Mount Goddard (Table 6.1). Maximum $\partial^{13}C$ values reached include +6.6 ‰ at Black Range Springs, -1.13 ‰ North Mount Goddard, +2.05 ‰ Bunyeroo Gorge and -0.08 ‰ at Devil's Peak (Table 6.2). The variations seen in the magnitude of this positive trend are thought to be a product of variable productivity and/or burial of organic matter.

Location	North Goddard	Black Range	Bunyeroo Gorge	Pichi Richi
Begining of shift	Unit 7/8	Unit 7/8	Unit 7/8	Unavailable
Maximum value	-1.1	6.6	2.05	-0.08

Table 6.2 Summary of positive isotopic shift, where it initiates and the maximum value reached

Two possible models are considered feasable for the production of this positive excursion.

In the first model, the isotopic excursion is thought to be associated with the formation of anoxic bottom waters in response to the development of a green-house Earth. These anoxic bottom waters will enhance the burial of organic matter, thus cutting off the supply of $^{12}CO_2$ to the bottom waters. The warming of these initially cold bottom waters will decrease the solubility of CO_2 in the water column, causing it to "bubble" out of the water. These two factors lead to the gradual equilibration of the "super-negative" bottom waters with the ^{13}C-enriched surface waters, and hence, cause a gradual increase in $\partial^{13}C$ values as this equillibrium is reached.

The second model involves the shallowing of the Wonoka ocean, and the deposition of shallow-water carbonate sequences. The positive isotopic excursion coincides with the

Figure 6.2

a) Glacial

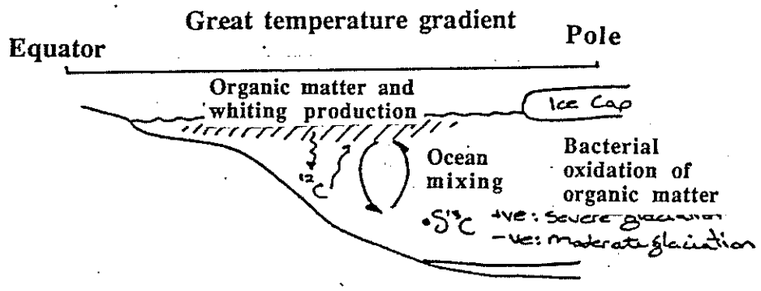

b) Post-Glacial

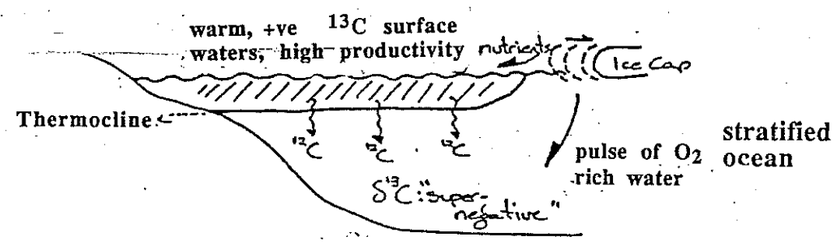

Formation of Wonoka Units 2-7

c) Greenhouse

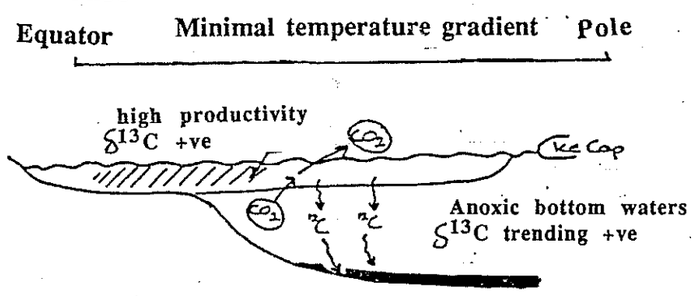

Super-negative signal is produced and maintained during b) by constant 'pumping' of ^{12}C (contained in organic matter) into the stratified bottomwaters. During c) anoxic bottom waters develop, preventing the bacterial oxidation of organic matter and hence cutting off supply of ^{12}C to the bottom waters. This, along with the preservation of organic matter, will cause a swing in the $\delta^{13}C$ to more positive values and gradual equllibration with isotopically heavy surface waters.

Figure 6.3

a) Unit 2 Formation

Erosion of basin edge initiates canyon incision

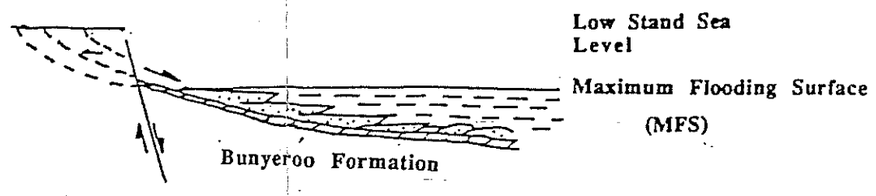

Unit 2: Is the product of erosional slumping (turbidity flows) along the basin edge, caused by an underfitting sea level and possibly associated with fault movement. Unit 2 represents a transgressive systems tract (TST). Canyon incision is initiated through the headward erosion of a faulted basin margin.

b) Unit 3-7 Formation

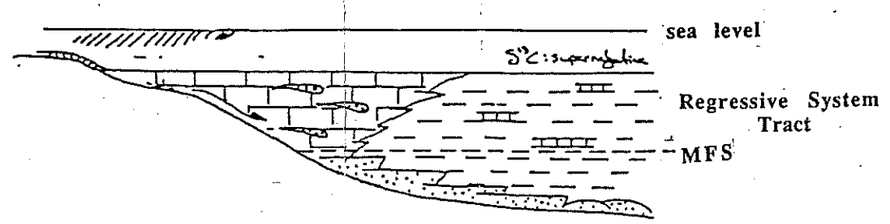

Canyon incision continues into Unit 3 development, canyons subsequently filled with later Wonoka Units.

c) Unit 8-11 Formation

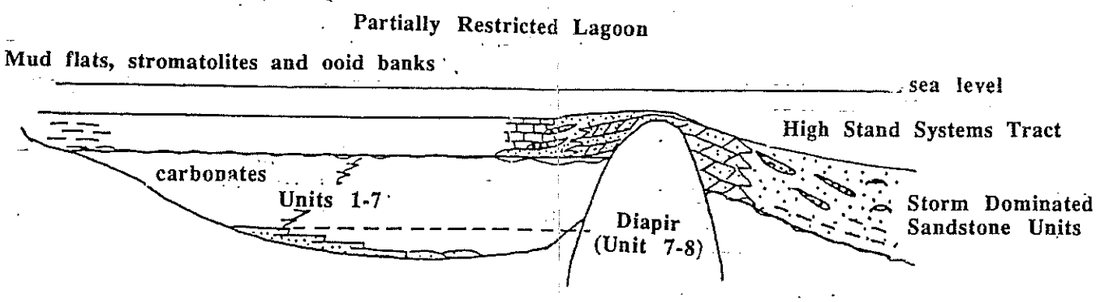

Formation of the positive carbon isotope excursion in the Upper Wonoka Formation, interpretted here to be a product of the fromation of a restricted lagoon and deposition in shallow water, $\delta^{13}C$ positive, photic zone, see text for details.

CHAPTER 7 STRONTIUM ISOTOPE SIGNAL

7.1 Theory and Sample Selection

Unlike the isotopes of carbon and oxygen, strontium isotopes in marine carbonates precipitate directly from the seawater, with no significant fractionation (Veizer, 1983; Derry et al., 1989; Asmerom et al., 1989, 1991; Kaufman et al., 1992). The $^{87}Sr/^{86}Sr$ ratio of seawater is controlled from inputs from two primary sources, the continental crust and the oceanic crust. The weathering, erosion and fluvial transport of continental material provides an isotopically heavy source for the oceanic reservoir, while the oceanic crust is a source of isotopically light Sr, through hydrothermal activity at the mid-oceanic ridge systems and the submarine alteration of basalts. It is the relative proportions of these two sources that will ultimately determine the strontium isotopic ratio of the seawater.

Of the four naturally occurring strontium isotopes two are of interest here: ^{87}Sr and ^{86}Sr, which comprise 7.04% and 9.87% of the strontium reservoir, respectively. ^{87}Sr is produced naturally by the radioactive decay of ^{87}Rb. Primary marine carbonates exclude ^{87}Rb from their lattice, so the primary Sr isotopic signal will remain unaltered in sedimentary carbonates through time, unless significant diagenetic influences have affected the rock. These influences tend to push $^{87}Sr/^{86}Sr$ ratios to higher values (Kaufman et al., 1992) and should be readily detectable when utilizing diagenetic tracers (Derry et al., 1989; Asmerom et al., 1991; Knoll, 1991; Derry et al., 1992; Kaufman et al., 1992).

Strontium has an oceanic residence time of approximately 4.5 Ma; and it takes roughly 1000 yrs to mix the oceans. Consequently, the $^{87}Sr/^{86}Sr$ ratio of the oceans at any one time is constant to within modern analytical precision (Veizer, 1983; Tucker and Wright, 1990; Asmerom et al., 1991; Kaufman et al., 1992). This, along with the fact no fractionation occurs with the incorporation of Sr into the carbonate lattice, makes variations in the $^{87}Sr/^{86}Sr$ ratio over geological history an extremely useful tool for high resolution stratigraphic correlations.

Altered carbonates have a higher Mn/Sr ratio than unaltered ones (Brand and Veizer, 1980). This is due to the strong partitioning of Mn into the carbonate phase during

carbonate-fluid interaction. Derry et al. (1992) found that higher $^{87}Sr/^{86}Sr$ values from all of their measured sections were associated with high Mn/Sr ratios. Thus, the Mn/Sr ratio is indeed a sensitive indicator of Sr isotopic alteration. Sr loss is significant during dolomitization because the distribution coefficient (K_d) between dolomite and water is smaller than that between calcite and water (indicating that if dolomitization occurs, the Sr will not re-enter the lattice of the precipitating dolomite phase as readily). Limestones have a better chance of maintaining a primary Sr isotopic signal than dolomites, even though they are more susceptible to alteration, because they contain considerably higher amounts of elemental Sr (Veizer et al., 1992). For this reason only limestones were considered for Sr isotope analysis, as dolomites have been found to be inadequate in diagenetic tracer studies (Asmerom et al., 1991).

The criteria used for screening out altered limestone samples were those adopted by other authors (Derry et al., 1989; Asmerom et al., 1991; Knoll, 1991; Derry et al., 1992; Kaufman et al., 1992). These criteria include:

1) low Mn/Sr ratios (<3)
2) no dolomitic component
3) no ^{87}Rb
4) relatively high Sr concentrations (preferably >500 ppm)
5) relatively positive $\partial^{13}C$ values (> 0 ‰PDB)

The use of these simple selection criteria during an initial screening excludes samples that show clear signs of alteration or contamination. However, samples that meet these tests are not necessarily usable in determining primary seawater $^{87}Sr/^{86}Sr$ values. Confidence in a given value for seawater is only justified when more than one sample from a particular interval gives the same result (Derry et al., 1992). Post-depositional alteration and exchange of Sr will result in elevated $^{87}Sr/^{86}Sr$ ratios. Thus when several samples of the same age yield different values, the lower values in the range are considered better estimates of the true $^{87}Sr/^{86}Sr$ value of the seawater at the time of deposition (Veizer and Compston, 1974; Derry et al., 1992).

The methods used for sample preparation, extraction of strontium and analysis for the relevant strontium isotopes are outlined in Appendix 5. A summary of the results is

presented in Table 7.1.

7.2 Discussion of Results

The carbonates of the Wonoka Formation are considered to have been originally aragonitic (Singh, 1986, 1987; Haines, 1987; DiBona, 1989). This is supported by the high Sr concentrations in many samples (up to 5,000 ppm) which indicate an aragonitic precursor (Derry et al., 1991).

No correlation between percentage yield and isotopic composition was found (Figure 7.1) indicating that no radiogenic Sr had been leached from the clastic phase of the samples (Derry et al., 1991). No detectable Rb was found in any samples, also indicating no input from the non-carbonate phase (see Appendix 5)

The samples from Black Range Springs showing the higher $^{87}Sr/^{86}Sr$ isotope values (A977-38, A977-40) are considered not to be representative of late Proterozoic seawater. This is because their high Ca/Sr ratios (2710 and 2209, respectively) indicate a large Sr loss, making them inappropriate for Sr isotope analysis (Asmerom et al., 1992), even though they have relatively low Mn/Sr ratios (1.100 and 1.860, respectively). The $^{87}Sr/^{86}Sr$ values of these samples are not consistent with other values obtained for the Wonoka Formation from Black Range Springs or North Mount Goddard, being significantly higher (by 0.01), and therefore possibly altered (Veizer and Compston, 1974; Derry et al., 1991). Sample A977-37 has a much lower Ca/Sr ratio (1313) and coincides well with samples analysed from North Goddard (A977-55 and A977-09) which also have relatively low Ca/Sr ratios of 348 and 1480, respectively. The low Mn/Sr ratios and high Sr contents of these three samples indicate that they give the best estimate of the seawater $^{87}Sr/^{86}Sr$ at the time of deposition of the mid-upper Wonoka Formation, namley 0.70936 to 0.70968. These values correspond with strontium isotopic ratios obtained by Ayliffe (1992) for the Wonoka carbonate platform sequence at Pichi Richi. With this value, and the Sr isotopic curve of Asmerom et al. (1991) (Figure 7.2), an approximate age for the Wonoka Formation can be estimated. The Wonoka Formation $^{87}Sr/^{86}Sr$ value falls just after the peak in the excursion to higher strontium isotope values at approximately 600 Ma. This indicates that the age of the mid- to upper-Wonoka Formation can be roughly estimated

at 560-590 Ma, which is in reasonable agreement with dates obtained by Christie -Blick et al. (1990) for Units 3 and 4 (viz. 580-630 Ma).

Sample No.	Meterage	87/86 Value	Mn ppm	Sr ppm	Mn/Sr	% Yield	Ca/Sr
North Mount Goddard							
977-55	630	0.709676	1082.6	1309	0.8	82.67	348
977-09	946	0.709592	249.4	239	1.0	39.70	1530
Black Range Springs							
977-37	623	0.709359	892.3	381	2.3	86.07	1313
977-38	689	0.710014	190.1	172	1.1	88.90	2710
977-40	754	0.710260	386.8	208	1.9	84.80	2209

Table 7.1 Summary of strontium isotopic analysis.

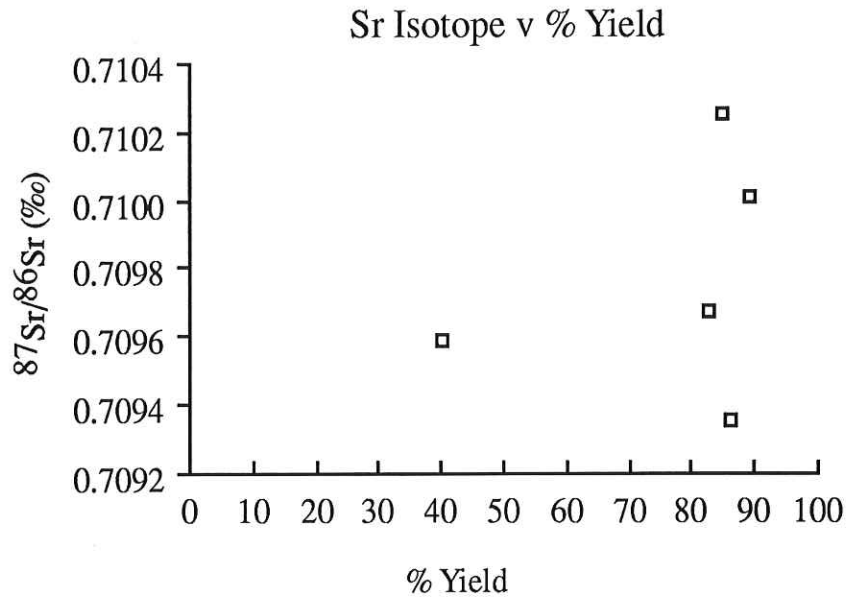

Figure 7.1 Plot of Sr isotopic values against % Yield, showing no correlation between the two variables.

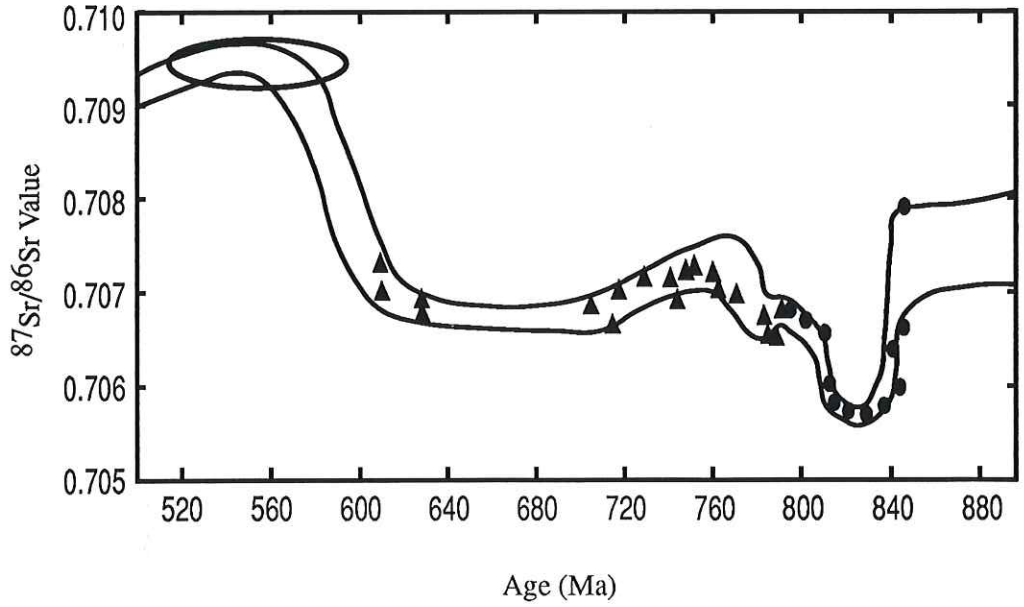

Figure 7.2 Strontium isotope curve and associated data points from Asmerom et al. (1991) showing the characteristic excursion to higher isotopic values begining at 600 Ma.. Outlined elipse represents the range of possible ages from isotopic values obtained in the present study.

CHAPTER 8 DISCUSSION AND CONCLUSIONS

It is often assumed that, given their age and associated likelihood of metamorphism, Proterozoic sedimentary rocks should be relatively poor candidates for carbon isotopic analysis. However, through careful sample selection, integrated with geochemical, petrographic and isotopic diagenetic analysis, carbonates of this age are as good as many of their Phanerozoic counterparts for this form of investigation.

The carbonates of the Wonoka Formation are not strongly affected by metamorphism (lower greenschist facies, chlorite zone: McKirdy et al., 1975) and contain very little organic matter (TOC values characteristically <0.05 wt %: Pell, 1989; Jansyn, 1990), thus reducing, or possibly even removing, the effects of thermal maturation of kerogens on the carbon isotopic composition of samples. This, in association with the fact that most of the carbonates observed in this study are either micritic limestones of low initial porosity, or show evidence of early lithification, reduces the diagenetic potential of the carbonates, making them less prone to diagenetic alteration.

In the present study two sections were analysed for carbon isotopes, namely North Mount Goddard and Black Range Springs. Carbon isotope values for these sections were validated by assessing the degree of alteration experienced by each individual sample, and determining the extent to which this alteration may, or may not, have affected the isotopic signal. Samples which were classified as altered were not included as part of the isotopic interpretation.

Curves obtained are readily correlatable with those produced by previous authors, namely, Jansyn (1990) for Bunyeroo Gorge, and Ayliffe (1992) for Pichi Richi, suggesting a possible primary origin for the observed isotopic trend. It was necessary that a model proposed to account for the formation of this curve contain an explanation of the great consistency seen within, and across, the formation. The presence of basinal waters containing an anomolously negative carbon isotopic signal during carbonate deposition was invoked to explain the Lower Wonoka Signal, with an origin for these isotopically light waters also being proposed. The positive trend has been interpreted to be the result of the shoaling of the sequence, and deposition of shallow-water carbonates.

A primary model has been proposed to explain the genesis of the Wonoka Formation isotopic signal, but diagenetic factors cannot be discounted. The rarity of such a consistent and negative signal, as that seen in the lower Wonoka Formation, may reflect either unique depositional and/or diagenetic conditions. Further research into such signals is essential before any valid judgement can be made as to their origin.

Acknowledgements

It would not be possible to express my gratitude to all people responsible for helping me see through this arduous year, but some cannot go without mention. I would firstly like to thank my family, whose most valued assistance, both financial and emotional, was crucial in keeping my spirits high and my feet on the ground. I must thank my field partner, Max, for providing an endless source of entertainment throughout our "fun" time in the field. My sincere thanks go to my supervisors, Dr. David McKirdy and Dr. Richard Jenkins, who provided the essential guidance required throughout the year, and who showed endless patience in the difficult task of coping with such a rag-tag team as Max and myself. The technical staff in the Department are the treasure of the Mawson, without their guidance I would have ended up as part of the jaw-crusher long ago, Thankyou. Last, but by no means least, goes my gratitude to my friend and companion Isobel, who made sure I was always in touch with reality.

Abbott, S.T. 1986. Stratigraphy and sedimentation of the Wilpena Group near Beltana Homestead, Central Flinders Ranges, South Australia. B.Sc. Honours thesis, Flinders University (unpub.).

Allan, J.R. and Matthews, R.K. 1982. Isotope signatures associated with early meteoric diagenesis. **Sedimentology**, v. 29, p. 797-817.

Asmeron, Y., Jacobsen, S.B., Knoll, A.H., Butterfield and Swett, K. 1991. Strontium isotopic variations of Neoproterozoic seawater: Implications for crustal evolution. **Geochimica et Cosmochimica Acta**, v. 55, p. 2883-2894.

Ayliffe, D.J. 1992. Geological setting of the late Proterozoic Wonoka Formation carbonate ramp and canyon sequence at Pichi Richi Pass Southern Flinders Ranges, South Australia: geochemical, stable isotope and diagenetic analysis. B.Sc. Honours thesis. University of Adelaide.

Battey, M.H. 1981. *Mineralogy for students, Second Edition.* Longman Scientific and Technical, England.

Berger, W.H. and Vincent, E. 1986. Deep sea carbonates: Reading the carbon-isotope signal. **Geologische Rundschau**, v. 75/1, p. 249-269.

Bone, Y., James, N.P. and Kyser, T.K. 1992. Synsedimentary detrital dolomite in Quaternary cool-water carbonate sediments, Lacepede shelf, South Australia. **Geology,** v. 20, p. 109-112.

Brand, U and Veizer, J. 1981. Chemical diagenesis of a multicomponent system-2: Stable isotopes. **Journal of Sedimentary Petrology,** v. 51, No. 3, p. 987-997.

Brand, U. and Veizer, J. 1980. Chemical diagenesis of a multicomponent carbonate system-1: Trace elements. **Journal of Sedimentary Petrology**, v. 50, No. 4, p. 1219-1236.

Brasier, M.D. 1992, Global ocean-atmospheric change across the Precambrian-Cambrian transition. **Geol. Mag.** v. 129, No. 2, p.161-168.

Abbott, S.T. 1986. Stratigraphy and sedimentation of the Wilpena Group near Beltana Homestead, Central Flinders Ranges, South Australia. B.Sc. Honours thesis, Flinders University (unpub.).

Allan, J.R. and Matthews, R.K. 1982. Isotope signatures associated with early meteoric diagenesis. **Sedimentology**, v. 29, p. 797-817.

Asmeron, Y., Jacobsen, S.B., Knoll, A.H., Butterfield and Swett, K. 1991. Strontium isotopic variations of Neoproterozoic seawater: Implications for crustal evolution. **Geochimica et Cosmochimica Acta**, v. 55, p. 2883-2894.

Ayliffe, D.J. 1992. Geological setting of the late Proterozoic Wonoka Formation carbonate ramp and canyon sequence at Pichi Richi Pass Southern Flinders Ranges, South Australia: geochemical, stable isotope and diagenetic analysis. B.Sc. Honours thesis. University of Adelaide.

Battey, M.H. 1981. *Mineralogy for students, Second Edition.* Longman Scientific and Technical, England.

Berger, W.H. and Vincent, E. 1986. Deep sea carbonates: Reading the carbon-isotope signal. **Geologische Rundschau**, v. 75/1, p. 249-269.

Bone, Y., James, N.P. and Kyser, T.K. 1992. Synsedimentary detrital dolomite in Quaternary cool-water carbonate sediments, Lacepede shelf, South Australia. **Geology,** v. 20, p. 109-112.

Brand, U and Veizer, J. 1981. Chemical diagenesis of a multicomponent system-2: Stable isotopes. **Journal of Sedimentary Petrology,** v. 51, No. 3, p. 987-997.

Brand, U. and Veizer, J. 1980. Chemical diagenesis of a multicomponent carbonate system-1: Trace elements. **Journal of Sedimentary Petrology**, v. 50, No. 4, p. 1219-1236.

Brasier, M.D. 1992, Global ocean-atmospheric change across the Precambrian-Cambrian transition. **Geol. Mag.** v. 129, No. 2, p.161-168.

Brasier, M.D., Anderson, M.M. and Corfield, R.M. 1992. Oxygen and carbon isotope stratigraphy of early Cambrian carbonates in southeastern Newfoundland and England. **Geol. Mag.** v. 129, No. 3, p. 265-279.

Brasier, M.D., Magaritz, M., Corfield, R. Huilin, L., Xiche, W., Lin, O., Zhiwen, J. Hamdi, B. Tinggui, H. and Fraser, A.G. 1990. The carbon- and oxygen-isotope record of the Precambrian-Cambrian boundary interval in China and Iran and their correlation. **Geol. Mag.,** v. 127, No. 4, p. 319-332.

Christie-Blick, N., von der Borch, C.C. and DiBona, P.A. 1990. Working Hypothesis for the origin of the Wonoka canyons (Neoproterozoic), South Australia. **American Journal of Science,** v. 290-A, p. 295-332.

Cloud, P.E. 1962. Environment of calcium carbonate deposition west of Andros Island, Bahamas. **U.S. Geol. Surv. Proff. Pap.** v. 350, p. 1-138.

Dalgarno, C.R. and Johnson, J.E. 1964. Wilpena Group. In Thomson B.P. et al., Precambrian rock froups in the Adelaide Geosyncline: a new subdivision. **Quart. geol. Notes. geol. Surv. S. Aust.** v. 20, p. 12-15.

Derry, L.A., Kaufman, A.J. and Jacobsen, S.B. 1992. Sedimentary cycling and environmental change in the Late Proterozoic: Evidence from stable and radiogenic isotopes. **Geochimica et Cosmochimica Acta,** v. 56, p. 1317-1329.

Derry, L.A., Keto, L.S., Jacobsen, S.B., Knoll A.H. and Swett, K. 1989. Sr isotope variations in Upper Proterozoic carbonates from Svalbard and east Greenland. **Geochimica et Cosmochimica Acta,** v. 53, p. 2331-2339.

DiBona, P.A. 1989. Geological history and sequence stratigraphy of the late Proteroic Wonoka Formation, northern flinders Ranges, South Australia. PhD Thesis, Flinders University.

DiBona, P.A., von der Borch, C.C. and Christie-Blick, N. 1990. Sequence stratigraphy and evolution of a basin-slope succession: The Late Proterozoic Wonoka Formation, Flinders Ranges, South Australia. **Journal of Earth Sciences,** v. 37, p. 135-145.

Brasier, M.D., Anderson, M.M. and Corfield, R.M. 1992. Oxygen and carbon isotope stratigraphy of early Cambrian carbonates in southeastern Newfoundland and England. **Geol. Mag.** v. 129, No. 3, p. 265-279.

Brasier, M.D., Magaritz, M., Corfield, R. Huilin, L., Xiche, W., Lin, O., Zhiwen, J. Hamdi, B. Tinggui, H. and Fraser, A.G. 1990. The carbon- and oxygen-isotope record of the Precambrian-Cambrian boundary interval in China and Iran and their correlation. **Geol. Mag.,** v. 127, No. 4, p. 319-332.

Christie-Blick, N., von der Borch, C.C. and DiBona, P.A. 1990. Working Hypothesis for the origin of the Wonoka canyons (Neoproterozoic), South Australis. **American Journal of Science,** v. 290-A, p. 295-332.

Cloud, P.E. 1962. Environment of calcium carbonate deposition west of Andros Island, Bahamas. **U.S. Geol. Surv. Proff. Pap.** v. 350, p. 1-138.

Dalgarno, C.R. and Johnson, J.E. 1964. Wilpena Group. In Thomson B.P. et al., Precambrian rock froups in the Adelaide Geosyncline: a new subdivision. **Quart. geol. Notes. geol. Surv. S. Aust.** v. 20, p. 12-15.

Derry, L.A., Kaufman, A.J. and Jacobsen, S.B. 1992. Sedimentary cycling and environmental change in the Late Proterozoic: Evidence from stable and radiogenic isotopes. **Geochimica et Cosmochimica Acta,** v. 56, p. 1317-1329.

Derry, L.A., Keto, L.S., Jacobsen, S.B., Knoll A.H. and Swett, K. 1989. Sr isotope variations in Upper Proterozoic carbonates from Svalbard and east Greenland. **Geochimica et Cosmochimica Acta,** v. 53, p. 2331-2339.

DiBona, P.A. 1989. Geological history and sequence stratigraphy of the late Proteroic Wonoka Formation, northern flinders Ranges, South Australia. PhD Thesis, Flinders University.

DiBona, P.A., von der Borch, C.C. and Christie-Blick, N. 1990. Sequence stratigraphy and evolution of a basin-slope succession: The Late Proterozoic Wonoka Formation, Flinders Ranges, South Australia. **Journal of Earth Sciences,** v. 37, p. 135-145.

Dott, R.H. (Jr) and Burgeois, J. 1982. Hummocky stratification; significance of its variable bedding sequences. **Geological Society of America Bulletin.** v. 93, p. 663-680.

Eickoff, K.H., von der Borch, C.C. and Grady, A.E. 1988. Proterozoic canyons of the Flinders Ranges (South Australia): submarine canyons or drowned river valleys? **Sedimentary Geology,** v. 58, p. 217-235.

Fairchild, I.J. and Spiro, B. Petrological and isotopic implications of some contrasting late Precambrian carbonates, NE Spitsbergen. **Sedimentology,** v. 34, p. 973-989.

Fairchild, I.J., Marshall, J.D., Bertand-Sarfati, J. 1990. Stratigraphic shifts in carbon isotopes from Proterozoic stromatilitic carbonates (Mauritonia): Influences of primary mineralogy and diagenesis. **American Journal of Science**, v. 290-A, p. 46-79.

Kirschvink, J.L. 1991. A palaeogeographic model for Vendian and Cambrian time, In Schopf, J.W., Klein, C. and Des Maris, D., Eds. **The Proterozoic biosphere: A multidisciplinary study:** Oxford, England, Oxford University Press.

Given, R.K. and Lohmann, K.C. 1985. Derivation of the original isotopic composition of Permian marine cements. **Journl of Sedimentary Petrology,** v. 55, No. 3, p. 430-439.

Grant, S.W.F. 1992. Carbon isotopic vital effect and organic diagenesis, lower Cambrian Forteau formation, northwest Newfoundland: Implications for Δ13C chemostratigraphy. **Geology**, v. 20, p. 243-246.

Haines, P.W. 1986. Late Proterozoic carbonate shelf to shale basin transition, Wonoka Formation, Flinders Ranges, S.A. 8th Australian Geological Convention, Adelaide, S.A., **Geological Society of Australia, Abstracts**, 15: 92-93.

Haines, P.W. 1988(a). A Late Proterozoic storm-dominated carbonate shelf sequence: The Wonoka formation in the central and southern Flinders Ranges, South Australia. **Geological Society of Australia, Special Publications** (in press).

Haines, P.W. 1988(b). Storm dominated mixed carbonate/siliciclastic shelf sequence displaying cycles of hummocky cross-stratification, late Proterzoic Wonoka Formation, South Asuatralia. **Sedimentary Geology**, v. 58, p. 237-254.

Hanford, C.R. 1986. Facies and sequences in shelf-storm-depositied carbonates-Fayetteville Shale and Pitkin Limestone (Mississippian) Arkansas. **Journal of Sedimentary Petrology**, v. 56, No. 1, p. 123-137.

Hoefs, J. 1987. *Stable Isotope Geochemistry, 3rd Edition.* Springer-Verlag, Berlin.

Hudson, J.D. 1977. Stable isotope and limestone lithification. **Journal of Geological Society of London,** v. 133, p. 637-660.

James, N.P. and von der Borch, C.C. 1991. Carbonate shelf edge off southern Australia: A prograding open-platform margin. **Geology**, v. 19, p. 1005-1008.

Jansen, E. 1989. The use of stable oxygen and carbon isotope stratigraphy as a dating tool. **Quaternary International**, v. 1, p. 151-166.

Jenkins, R.J.F. and Gostin, V.A. 1983. Marinoan and Ediacaran type sections in the context of tectonic cycles in the Adelaide Geosyncline. Adelaide Geosyncline Sedimentary Environments and Tectonic Setting Symposium, Adelaide. **Geol. Soc. Aust. Abs.** v. 10, p 39-44.

Jenkins, R.J.F., McKirdy, D.M., Foster, C.B., O'Leary, T. and Pell, S.D. 1991. **Geological Magazine**, v.129 (in press).

Kaufman, A.J., Hayes, J.M., Knoll, A.H. and Germs, G.J.B. 1991. Isotopic compositions of carbonates and organic carbon from upper Proterozoic successions in Namibia: stratigraphic variation and the effects of diagenesis and metamorphism. **Precambrian Research,** v. 49, p. 301-327.

Kaufman, A.J., Knoll, A.H. and Awranik, S.M. 1992. Biostratigraphic and chronostratigraphic correlation of Neoproterozoic sedimentary successions: Upper Tindir Group, north-western Canada, as a test case. **Geology**, v. 20 p.181-185.

Haines, P.W. 1988(b). Storm dominated mixed carbonate/siliciclastic shelf sequence displaying cycles of hummocky cross-stratification, late Proterzoic Wonoka Formation, South Asuatralia. **Sedimentary Geology**, v. 58, p. 237-254.

Hanford, C.R. 1986. Facies and sequences in shelf-storm-depositied carbonates-Fayetteville Shale and Pitkin Limestone (Mississippian) Arkansas. **Journal of Sedimentary Petrology**, v. 56, No. 1, p. 123-137.

Hoefs, J. 1987. *Stable Isotope Geochemistry, 3rd Edition.* Springer-Verlag, Berlin.

Hudson, J.D. 1977. Stable isotope and limestone lithification. **Journal of Geological Society of London,** v. 133, p. 637-660.

James, N.P. and von der Borch, C.C. 1991. Carbonate shelf edge off southern Australia: A prograding open-platform margin. **Geology**, v. 19, p. 1005-1008.

Jansen, E. 1989. The use of stable oxygen and carbon isotope stratigraphy as a dating tool. **Quaternary International**, v. 1, p. 151-166.

Jenkins, R.J.F. and Gostin, V.A. 1983. Marinoan and Ediacaran type sections in the context of tectonic cycles in the Adelaide Geosyncline. Adelaide Geosyncline Sedimentary Environments and Tectonic Setting Symposium, Adelaide. **Geol. Soc. Aust. Abs.** v. 10, p 39-44.

Jenkins, R.J.F., McKirdy, D.M., Foster, C.B., O'Leary, T. and Pell, S.D. 1991. **Geological Magazine**, v.129 (in press).

Kaufman, A.J., Hayes, J.M., Knoll, A.H. and Germs, G.J.B. 1991. Isotopic compositions of carbonates and organic carbon from upper Proterozoic successions in Namibia: stratigraphic variation and the effects of diagenesis and metamorphism. **Precambrian Research,** v. 49, p. 301-327.

Kaufman, A.J., Knoll, A.H. and Awranik, S.M. 1992. Biostratigraphic and chronostratigraphic correlation of Neoproterozoic sedimentary successions: Upper Tindir Group, north-western Canada, as a test case. **Geology**, v. 20 p.181-185.

Knoll, A.H., Hayes, J.M., Kaufman, A.J. Swett, K. and Lambert I.B. 1986. Secular variations in carbon isotope ratios from Upper Proterozoic successions of Svalbard and east Greenland. **Nature**, v. 321, p. 832-835.

Lambert, I.B. and Donnelly, T.H. 1991. Atmospheric oxygen levels in the Precambrian: a review of isotopic and geological evidence. **Palaeogeography, Palaeoclimatology, Palaeoecology (Global and Planetary Change Section)**, v. 97, p. 83-91.

Lambert, I.B., Walter, M.R., Wenlong, Z., Songnian, L. and Guogan, M. 1987. Palaeoenvironmental and carbon isotope stratigraphy of Upper Proterozoic carbonates of the Yangtzee Platform. **Nature**, v. 325, p. 140-142.

Magaritz, M. 1975, Sparitization of a pelleted limestone: A case study of carbon and oxygen isotopic composition. **Journal of Sedimentary Petrology,** v. 45, No. 3, p. 599-603.

Magaritz, M. 1983. Carbon and oxygen isotope composition of recent and ancient coated grains. In Peryt, T.M. 1983. *Coated Grains*. Springer-Verlag Berlin.

Magaritz, M. 1989. ^{13}C minima follow extinction events: A clue to faunal radiation. **Geology**, v. 17, p. 337-340.

Magaritz, M. 1990. Carbon isotopes, time boundaries and evolution. **Terra Nova**, v. 3, p. 251-256.

Magaritz, M., H., Bar, R., Baud, A. and Holser, W.T. 1988. The C-isotope shift at the Permian/Triassic boundary in the southern Alps is gradual. **Nature**, v. 331, p. 337-339.

Magaritz, M., Holser, W.T. and Kirschvink, J.L. 1986. Carbon isotope events across the Precambrian/Cambrian boundary on the Siberian Platform. **Nature**, v. 320, p. 258-259.

Magaritz, M., Kirschvink, J.L., Latham, A.J., Zhuravlev, A.Y. and Rozanov, A.Y. 1991. Precambrian/Cambrian boundary problem: Carbon isotope correlations for Vendian and Tommotian time between Siberia and Morocco. **Geology**, v. 19, p. 847-850.

Knoll, A.H., Hayes, J.M., Kaufman, A.J. Swett, K. and Lambert I.B. 1986. Secular variations in carbon isotope ratios from Upper Proterozoic successions of Svalbard and east Greenland. **Nature**, v. 321, p. 832-835.

Lambert, I.B. and Donnelly, T.H. 1991. Atmospheric oxygen levels in the Precambrian: a review of isotopic and geological evidence. **Palaeogeography, Palaeoclimatology, Palaeoecology (Global and Planetary Change Section)**, v. 97, p. 83-91.

Lambert, I.B., Walter, M.R., Wenlong, Z., Songnian, L. and Guogan, M. 1987. Palaeoenvironmental and carbon isotope stratigraphy of Upper Proterozoic carbonates of the Yangtzee Platform. **Nature**, v. 325, p. 140-142.

Magaritz, M. 1975, Sparitization of a pelleted limestone: A case study of carbon and oxygen isotopic composition. **Journal of Sedimentary Petrology,** v. 45, No. 3, p. 599-603.

Magaritz, M. 1983. Carbon and oxygen isotope composition of recent and ancient coated grains. In Peryt, T.M. 1983. *Coated Grains*. Springer-Verlag Berlin.

Magaritz, M. 1989. ^{13}C minima follow extinction events: A clue to faunal radiation. **Geology**, v. 17, p. 337-340.

Magaritz, M. 1990. Carbon isotopes, time boundaries and evolution. **Terra Nova**, v. 3, p. 251-256.

Magaritz, M., H., Bar, R., Baud, A. and Holser, W.T. 1988. The C-isotope shift at the Permian/Triassic boundary in the southern Alps is gradual. **Nature**, v. 331, p. 337-339.

Magaritz, M., Holser, W.T. and Kirschvink, J.L. 1986. Carbon isotope events across the Precambrian/Cambrian boundary on the Siberian Platform. **Nature**, v. 320, p. 258-259.

Magaritz, M., Kirschvink, J.L., Latham, A.J., Zhuravlev, A.Y. and Rozanov, A.Y. 1991. Precambrian/Cambrian boundary problem: Carbon isotope correlations for Vendian and Tommotian time between Siberia and Morocco. **Geology**, v. 19, p. 847-850.

Marshall, J.D. 1992. Climatic and oceanographic isotope signals from the carbonate rock record and their preservation. **Geological Magazine**, v. 129 (2), p. 143-160.

McNaughton, N.J., and Withnall, I.W. 1985. Carbonate ^{13}C and ^{18}O depletion during regional metamorphism. In Herbert, H.K, and Ho, S.E. 1990. **Stable Isotopes and Fluid Processes in Mineralization**. Publication No. 23, Geology Department and University Espension, University of Western Australia.

Pell, S. 1989. Stable isotope composition of organic matter and co-existing carbonate in the Late Precambrian of the Officer basin: Stratigrapnic relationships with neighbouring basins and environmental significance. Honours Thesis, Adelaide University.

Plummer, P.S. 1978. Stratigraphy of the lower Wilpena Group (late Precambrian), Flinders Ranges, South Australia. **Trans. R. Soc. S. Aust.,** v. 102, p. 25-38.

Reijmer, J.J.G., Tenkate, W.G.H.Z., Sprenger, A. and Schlager, W. 1991. Calciturbidite composition related to exposure and flooding of a carbonate platform (Triassic, Eastern Alps). **Sedimentology**, v. 38, p. 1059-1074.

Robbins, L.L. and Blackwelder, P.L. 1992. Biochemical and ultrastructural evidence for the origin of whitings: A biologically induced calcium carbonate precipitation mechanism. **Geology,** v. 20, p. 464-468.

Schidlowski, M. 1988. A 3,800-million-year isotopic record of life from carbon in sedimentary rocks. **Nature**, v. 333, p. 313-318.

Scotford, G.L. 1984. Sedimentation of Late Proterozoic sediments with syn-depsotional diapirism, and Delamerian thrust faulting, Warraweena, northern Flinders Ranges, South Australia. Honnours Thesis, University of Adelaide.

Shinn, E. A., Steinen, R.P., Lidz, B.H. and Swart, P.K. 1989. Perspectives: Whitings, a sedimentologic dilemma. **Journal of Sedimentary Petrology**, v. 59, No. 1, p. 147-161,

Sibley, D.F. and Gregg, J.M. 1987. Classification of dolomite rock textures. **Journal of Sedimentary Petrology**, v. 57, p. 967-975.

Marshall, J.D. 1992. Climatic and oceanographic isotope signals from the carbonate rock record and their preservation. **Geological Magazine**, v. 129 (2), p. 143-160.

McNaughton, N.J., and Withnall, I.W. 1985. Carbonate ^{13}C and ^{18}O depletion during regional metamorphism. In Herbert, H.K, and Ho, S.E. 1990. **Stable Isotopes and Fluid Processes in Mineralization**. Publication No. 23, Geology Department and University Espension, University of Western Australia.

Pell, S. 1989. Stable isotope composition of organic matter and co-existing carbonate in the Late Precambrian of the Officer basin: Stratigrapnic relationships with neighbouring basins and environmental significance. Honours Thesis, Adelaide University.

Plummer, P.S. 1978. Stratigraphy of the lower Wilpena Group (late Precambrian), Flinders Ranges, South Australia. **Trans. R. Soc. S. Aust.,** v. 102, p. 25-38.

Reijmer, J.J.G., Tenkate, W.G.H.Z., Sprenger, A. and Schlager, W. 1991. Calciturbidite composition related to exposure and flooding of a carbonate platform (Triassic, Eastern Alps). **Sedimentology**, v. 38, p. 1059-1074.

Robbins, L.L. and Blackwelder, P.L. 1992. Biochemical and ultrastructural evidence for the origin of whitings: A biologically induced calcium carbonate precipitation mechanism. **Geology,** v. 20, p. 464-468.

Schidlowski, M. 1988. A 3,800-million-year isotopic record of life from carbon in sedimentary rocks. **Nature**, v. 333, p. 313-318.

Scotford, G.L. 1984. Sedimentation of Late Proterozoic sediments with syn-depsotional diapirism, and Delamerian thrust faulting, Warraweena, northern Flinders Ranges, South Australia. Honnours Thesis, University of Adelaide.

Shinn, E. A., Steinen, R.P., Lidz, B.H. and Swart, P.K. 1989. Perspectives: Whitings, a sedimentologic dilemma. **Journal of Sedimentary Petrology**, v. 59, No. 1, p. 147-161,

Sibley, D.F. and Gregg, J.M. 1987. Classification of dolomite rock textures. **Journal of Sedimentary Petrology**, v. 57, p. 967-975.

Singh, U. 1986. Late Precambrian and Cambrian carbonates of the Adelaidean in the Flinders Ranges, South Australia - A Petrographic, electron microprobe and stable isotope study. PhD thesis at University of Adelaide.

Singh, U. 1987. Ooids and cements from the late Precambrian of the Flinders Ranges, South Australia. **Journal of Sedimentary Petrology**, v. 57, No. 1, p. 117-12

Sukonata, U., Thomas, B., Von der Borch, C.C. and Gatehouse, C.G. 1991. Sequence stratigraphic studies and canyon formation, South Australia. **PESA Journal**, p. 68-73.

Sweeny, R.E. and Kaplan, J.R. 1973. Pyrite framboid formation: Laboratory synthesis and marine sediments. **Economic Geology**, v. 68, p. 618-634.

Tucker, M.E. 1990. Carbon isotopes and Precambrian-Cambrian geology, South Australia: Ocean basin formation, seawater chemistry and organic evolution. **Terra Nova**, v. 1, p. 573-582.

Tucker, M.E. and Wright, V.P. 1990. *Carbonate Sedimentology*. Blackwell Scientific Publications, Oxford.

Veiser, J., Compston, W., Clauer, N. and Schidlowski, M. 1983. 87Sr/86Sr in late Proterozoic carbonates; Evidence for a "mantle event" at 900 Ma ago. **Geochimica et Cosmochimica Acta**, v. 47, p. 295-302.

Veizer, J. and Hoefs, J. 1976. The nature of 18O/16O and 13C/12C secular trends in sedimentary carbonate rocks. **Geochimica et Cosmochimica Acta**, v. 40, p. 1387-1395.

Veizer, J., Fritz, P. and Jones, B. 1986. Geochemistry of brachiopods: Oxygen and carbon isotopic records of Paleozoic oceans. **Geochim. et Cosmochim. Acta**, v. 50, p. 16791696.

Veizer, J., Holser, W.T. and Wigus, C.K. 1980. Correlation of 13C/12C and 34S/32S secular variations. **Geochimica et Cosmochimca Acta**, v. 44, p. 579-587.

Singh, U. 1986. Late Precambrian and Cambrian carbonates of the Adelaidean in the Flinders Ranges, South Australia - A Petrographic, electron microprobe and stable isotope study. PhD thesis at University of Adelaide.

Singh, U. 1987. Ooids and cements from the late Precambrian of the Flinders Ranges, South Australia. **Journal of Sedimentary Petrology**, v. 57, No. 1, p. 117-12

Sukonata, U., Thomas, B., Von der Borch, C.C. and Gatehouse, C.G. 1991. Sequence stratigraphic studies and canyon formation, South Australia. **PESA Journal**, p. 68-73.

Sweeny, R.E. and Kaplan, J.R. 1973. Pyrite framboid formation: Laboratory synthesis and marine sediments. **Economic Geology**, v. 68, p. 618-634.

Tucker, M.E. 1990. Carbon isotopes and Precambrian-Cambrian geology, South Australia: Ocean basin formation, seawater chemistry and organic evolution. **Terra Nova**, v. 1, p. 573-582.

Tucker, M.E. and Wright, V.P. 1990. *Carbonate Sedimentology*. Blackwell Scientific Publications, Oxford.

Veiser, J., Compston, W., Clauer, N. and Schidlowski, M. 1983. 87Sr/86Sr in late Proterozoic carbonates; Evidence for a "mantle event" at 900 Ma ago. **Geochimica et Cosmochimica Acta**, v. 47, p. 295-302.

Veizer, J. and Hoefs, J. 1976. The nature of 18O/16O and 13C/12C secular trends in sedimentary carbonate rocks. **Geochimica et Cosmochimica Acta**, v. 40, p. 1387-1395.

Veizer, J., Fritz, P. and Jones, B. 1986. Geochemistry of brachiopods: Oxygen and carbon isotopic records of Paleozoic oceans. **Geochim. et Cosmochim. Acta**, v. 50, p. 16791696.

Veizer, J., Holser, W.T. and Wigus, C.K. 1980. Correlation of 13C/12C and 34S/32S secular variations. **Geochimica et Cosmochimca Acta**, v. 44, p. 579-587.

von der Borch, C.C. 1980. Evolution of late Proterozoic to early Paleozoic Adelaide Foldbelt, Australia: comparisons with post-Permian rifts and passive margins. **Tectonophysics**, v. 70, p. 115-134.

von der Borch, C.C. and Grady, A.E. 1984. Mechanisms of sandstone deposition in a late Proterozoic submarine canyon, Adelaide Geosyncline, South Australia. **Bull. Am. Ass. Petrol. Geol.** v. 68, p. 684-689.

von der Borch, C.C., Christie-Blick, N. and Grady, A.E. 1988. Depositional sequence analysis applied to late Proterozoic Wilpena Group, Adealide Geosyncline, south Australia. **Australian Journal of Earth Sciences,** v. 35, p. 59-71.

von der Borch, C.C., Smitt, R. and Grady, A.E. 1982. Late Proterozoic submarine canyons of the Adelaide Geosyncline, South Australia. **Am. Ass Petrol. Geol. Bull.,** v. 66, p. 332-347.

Walker, R.G. (Ed.) 1984. *Facies Models, Second Edition.* Ainsworth Press Limited, Ontario.

Walker, R.G., Duke, W.L. and Leckie, D.A. 1983. Hummocky stratification: Significance of its variable bedding sequences: Discussion and reply. **Geological Society of America Bulletin**, v. 94, p. 1245-1251.

Weissert, H. 1989. C-Isotope stratigraphy, a monitor of paleoenvironmental change: A case study from the Early Cretaceous. **Surveys in Geophysics**, v. 10, p. 1-61.

Weissert, H. and Channell, J.E.T. 1989. Tethyan carbonate carbon isotope stratigraphy across the Jurassic-Cretaceous boundary: An indicator of decelerated global carbon cycling? **Paleoceanography**, v. 4, No. 4, p. 483-494.

Wetzel, A. and Balson, P. 1992. Sedimentology of fine grained turbidites inferred from continuously recorded physical properties data. **Marine Geology**, v. 104, p. 165-178.

Williams, D.F. and Trainor, D. 1986. Application of isotope chronostratigraphy in the noerthern Gulf of Mexico. **Gulf Coast Association of Geological Societies-Transactions**, v. 36, p. 589-599.

von der Borch, C.C. 1980. Evolution of late Proterozoic to early Paleozoic Adelaide Foldbelt, Australia: comparisons with post-Permian rifts and passive margins. **Tectonophysics**, v. 70, p. 115-134.

von der Borch, C.C. and Grady, A.E. 1984. Mechanisms of sandstone deposition in a late Proterozoic submarine canyon, Adelaide Geosyncline, South Australia. **Bull. Am. Ass. Petrol. Geol.** v. 68, p. 684-689.

von der Borch, C.C., Christie-Blick, N. and Grady, A.E. 1988. Depositional sequence analysis applied to late Proterozoic Wilpena Group, Adealide Geosyncline, south Australia. **Australian Journal of Earth Sciences,** v. 35, p. 59-71.

von der Borch, C.C., Smitt, R. and Grady, A.E. 1982. Late Proterozoic submarine canyons of the Adelaide Geosyncline, South Australia. **Am. Ass Petrol. Geol. Bull.,** v. 66, p. 332-347.

Walker, R.G. (Ed.) 1984. *Facies Models, Second Edition.* Ainsworth Press Limited, Ontario.

Walker, R.G., Duke, W.L. and Leckie, D.A. 1983. Hummocky stratification: Significance of its variable bedding sequences: Discussion and reply. **Geological Society of America Bulletin**, v. 94, p. 1245-1251.

Weissert, H. 1989. C-Isotope stratigraphy, a monitor of paleoenvironmental change: A case study from the Early Cretaceous. **Surveys in Geophysics**, v. 10, p. 1-61.

Weissert, H. and Channell, J.E.T. 1989. Tethyan carbonate carbon isotope stratigraphy across the Jurassic-Cretaceous boundary: An indicator of decelerated global carbon cycling? **Paleoceanography**, v. 4, No. 4, p. 483-494.

Wetzel, A. and Balson, P. 1992. Sedimentology of fine grained turbidites inferred from continuously recorded physical properties data. **Marine Geology**, v. 104, p. 165-178.

Williams, D.F. and Trainor, D. 1986. Application of isotope chronostratigraphy in the noerthern Gulf of Mexico. **Gulf Coast Association of Geological Societies-Transactions**, v. 36, p. 589-599.

Winter, B.L. and Knauth, L.P. 1992. Stable isotope geochemistry of early Proterozoic carbonate concretions in the Animikie Group of the Lake Superior region; Evidence for anaerobic bacterial processes. **Precambrian Research**, v. 54, p. 131-151.

Veizer, J. 1983. Chemical diagenesis of carbonates: Theory and application, In Arthur, M.A. et al., Eds. *Stable Isotopes in Sedimentary Geology*: Society of Economic Palaeontologists and Mineralogists Short Course No. 10. p. 3.1-3.100.

Anderson, T.F. and Arthur, M.A. 1983. Stable isotopes of oxygen and carbon and their application to sedimentologic and paleoenvironmental problems, In Arthur, M.A. et al., Eds. *Stable Isotopes in Sedimentary Geology*: Society of Economic Palaeontologists and Mineralogists Short Course No. 10. p 1.1-1.151.

LIST OF APPENDICES

APPENDIX 1

ANALYTICAL METHODS

Analysis carried out on collected field samples include:

1.1) Total Carbon Determination (LOI)

1.2) X-Ray Diffraction

1.3) Carbonate Staining

1.4) Cathodoluminescence

1.5) Atomic Absorbtion Spectroscopy

1.6) Strontium Isotope Determination

1.7) Sulphur Isotope Determination

1.8) Whole rock calcite and dolomite $\partial^{18}O$ and $\partial^{13}C$ determination.

1.1 Total Carbon Determination

Organic/Inorganic carbon content was determined by following the procedure outlined by the Loss on Ignition program supplied by Phil McDuie.

1) 3-4 g of finely powdered sample were weighed into a clean glass vial using the Sartorius R200D Dual Range Electronic Balance.

2) Samples were then placed into a 110°C oven for drying. After a minimum period of 4 hrs the samples were removed and placed into a desiccator and allowed to cool to room temperature.

3) The Sharp PC-4502 computer was connected to the Sartorius Balance and the SEDLOSS program run.

4) Samples were placed into pre-weighed alumina crucibles and weighed. This inital sample + crucible weight was then logged into the computer.

5) The weighed samples were then put into a silica tray and placed into a muffle furnace for ignition at 500°C for one hour.

6) After one hour the samples were removed and placed into a desiccator to cool to room temperature.

7) The samples were re-weighed and the percentage of the weight lost was calculated. This percentage loss was taken to be the organic carbon content of the sample.

8) The samples were placed back into the silica tray and put in the muffle furnace for ignition at 1000°C for one hour.

9) Once ignition was complete, samples were removed from the furnace and allowed to cool for 15 minutes before being placed into the desiccator to cool to room temperature.

10) The samples were then re-weighed and the percentage weight lost calculated. This percentage loss was taken to be the carbonate carbon content of the sample.

11) The two ignition values were combined to give an estimate of the total carbon content of the samples.

1.2 X-Ray Diffraction

Sample preparation procedure for XRD analysis was as follows:

1) A small amount of finely ground sample was mixed with 3-4 drops of deionized water in a mortar and pestle to form a paste.

2) This paste was then spread evenly over a clean dry slide and dried in an oven at 115°C.

3) The slide was analysed in a Siemens X-Ray Diffractometer using a Cu K_α target at 35mA and 50kV, set at 0.5° in and 0.5° out at a scan speed of 1°/min at 1000 cps full scale deflection using quartz as the standard.

4) These sample XRD plots were then used to determine the dolomite percentage of each sample.

Percentage Dolomite Determination

1) The principle XRD peaks of dolomite and calcite (ie. calcite då = 3.03 ; dolomite då = 2.89) were corrected for background 'noise'.

2) The ratio between the calcite peak and the dolomite peak was calculated.

3) This value was then plotted on a graph for percentage dolomite determination provided by Mr Nick Lemon (NCPGG) constructed on data obtained by Tennet and Berger (1957) and Singh (1983).

1.3 Carbonate Staining

The staining method outlined by Dickson (1965) was followed for the staining of thin sections and hand samples.

Staining solutions were prepared in the following manner:

1) Alizarin Red S (.2gm) was dissolved in 100 ml of 1.5% HCl.

2) Potassium Ferrycyanide (2.0gm) was dissolved in 100 ml of 1.5% HCl.

3) These two solutions were mixed in a 3:2 ratio of Alizarin Red to Potassium Ferrycyanide in a large petri dish to produce the staining solution.

One side of all thin sections and a couple of polished hand specimens were stained using these solutions in the following way:

1) The slide/hand specimen was etched in 1.5% HCl for 15-20 seconds, then rinsed in deionized water.

2) The slide/hand specimen was then immersed the staining solution for 45 seconds, any excess staining solution was washed off with deionized water.

3) The sample was then immersed in acidified alizarin Red S solution for 10-15 seconds and rinsed again.

4) The sample was then set aside to dry.

Colours for the Determination of Carbonate:

1) Dolomite - colourless
2) Calcite - pale pink to red
3) Ferroan Calcite - mauve to purple to royal blue
4) Ferroan Dolomite - pale to deep turquoise

1.4 Cathodoluminescence (CL)

Polished thin sections were made of all samples that were analysed. These were first petrographically analysed and those showing recrystallization and/or dolomitization were then viewed under CL. Photographs were taken of a few selected slides that showed information of interest under the following conditions:

CL Conditions:

- 18-20 KV
- 200-220 mA
- Reciprocity Failure Correction : 4
- Light/Dark Field Correction : D80%

Photographic Conditions:

-1-15 second exposure time
- Exktapress ppc 1600 film

1.5 Atomic Absorbtion Spectroscopy

All samples that were analysed for carbon and oxygen isotopes were analysed using AAS. Each sample was analysed for a total of six elements, which included magnesium, manganese, iron, calcium, strontium and rubidium.

Sample Preparation

Dissolution of samples was done using a method based on the procedure described by Derry et al (1992). This involved using acetic acid, instead of the generally accepted HCl, to dissolve the sample. This is done to target the carbonate component for dissolution and to leave the clastic and clay components undissolved. The procedure was as follows:

1) Approximately 1gm of finely powdered sample was weighed into a clean teflon beaker using the Sartorius R200D Dual Range Electronic Balance. A standard limestone sample (JLs-1) and standard dolomite (JDo-1) were also measured as well as a blank for comparison.

2) The samples were then "wetted" with a small amount of deionized water to prevent excessive effervessing.

3) 20 ml of 5N acetic acid was then added, and the beaker placed on a hot plate at 60°C.

4) After a reaction time of three hours the hot plate was turned up to 110°C and the samples were left overnight to evapourate to dryness.

5) Once evapouration was complete, 10 ml of 5N acetic acid was added to redissolve the residue.

6) 10 ml of La/K solution (2% wt in .5M HCl) was added to each beaker immediately before filtering with Whatmans 52 hardened 11cm filter paper.

7) This filtered solution was then made up to 100 ml for AAS analysis.

8) All sample solutions were also diltued down twenty times by adding 5 ml of the sample solution with 9.5 ml of the La/K solution and 9.5 ml of 5N acetic acid and making the solution up to 100 ml, to keep the same acid concentrations. It was neccessary to use this diluted solution for the analysis of

some elements (such as calcium and magnesium) due to their great abundance in some samples.

Analysis of Samples

All analysis was done on the Varian AA-6 Atomic Absorbtion Spectrometer using an air/acetylene flame and appropriate hollow cathode lamps for the required elements. All samples were measured at least three times, as were the three standards of known concentrations. The parts per million values of each sample were determined by using the Multi Element program for AAS Analysis, supplied by Phil McDuie. All results were corrected back to give ppm values for the dissolved carbonate portion of the sample by using the Total Carbonate Content values obtained by the Loss on Ignition procedure described previously.

1.6 Strontium Isotope Determination

Samles were selected for Strontium analysis following the selection criteria as outlined by Kaufman et al (1992). Samples with low Mn/Sr ratios, little or no Rb, no dolomite portion and high $\partial^{13}C$ vlaues were targetted for strontium analysis. These selected samples were prepared in the following way:

1) Approximately 100 mg of sample was dissolved in a clean teflon beaker in 8 ml of 1N HCl for one hour.

2) Approximately 6-7 ml of the solution was pipetted off, being careful to avoid collecting any solid fraction.

3) This solution was put into a clean centrifuge tube and centrifuged for 5 minutes at 3000 rpms in a Clements GS1000 centrifuger.

4) 5-6 ml of this centrifuged solution was pipetted off and placed in a second clean centrifuge tube and centrifuged a second time.

5) Approximately 5 ml of this solution was pipetted off and put into a clean teflon beaker, which was then placed on a hotplate at 180°C to evapourate dry.

6) The solid fraction that was left after comnplete evapouration of the acid was then redissolved in 1.5 ml of 3N HCl and put through the columns following the procedure outlined for strontium IC analysis.

7) The solution collected from this procedure was then put on the hotplate to evapourate to dryness at 180°C.

8) The solid fraction formed was then dissolved with 1µl of H_3PO_4 and placed onto a single tantalum filament (which has 1µl of H_3PO_4 evapourated on it) and evapourated dry.

9) Filament holder and side and extraction plate were then mounted onto the sample magazine.

Strontium Isotope Analysis

1) Samples were analysed on the Finnigan MAT261 Mass Spectrometer.

2) The program Sr IC Expt 7:H6,0,3 was used, analysing for the strontium isotopes ^{85}S, ^{86}S, ^{87}S and ^{88}S and was run manually.

1.5 Sulphur Isotope Determination

Pyrite, chalcopyrite and galena were found in certain levels of the Wonoka Formation, these ranged from finely disseminated, framboidal occurrences, to both small and large (.5-3mm) crystals and to veins of sulphides.

Sample Preparation

The sulphide samples were extracted from the limestone using a dentist drill and the SO_2 generated in the following way:

1) The sample was weighed out accurately using the Sartorius R200D Dual Range Electronic Balance

2) This was then placed in a ceramic boat along with 120 mg of Cu_2O.

3) The sample was then heated to 950°C in a furnace under vacuum for approximately 12 minutes.

4) The evolved gas was separated into condensables and non-condensables by means of freezing with liquid nitrogen to remove the non-condensables.

5) The water vapour was then extracted using a cold ethanolsolution, while the remainder was collected by freezing once again with liqud nitrogen.

6) CO_2 and SO_2 were separated using a slurry tap of n-penthane, with the SO_2 then being collected in a glass tube by freezing with liquid nitrogen.

7) The glass tube was then sealed by means of an oxy-acetalene torch.

Sulphur Isotope Measurement

The SO_2 gas collected was measured on a Micromass VG 602E Stable Isotope Mass Spectrometer. The ratios of $^{34}S/^{32}S$ were compared with the international standard Canyon Diablo Triolite (CDT). The results are quoted as $\partial^{34}S$ values and expressed in parts per thousand (‰).

1.8 Whole Rock $\partial^{13}C$ and $\partial^{18}O$ Determination

Using the data obtained from the XRD analysis, the samples were grouped according to dolomite content. Samples with <15% dolomite component were analysed

following the "Calcite Procedure" described below. Those samples classed as "mixed", ie. containing ≥15% dolomite ≤ 85% were analysed following the "Mixed Carbonate Procedure" described below and those samples with >85% dolomite were treated as pure dolomite samples and were analysed following the "Dolomite Procedure" as described below.

Sample Preparation

1) The carbonate sample to be analysed was removed from the hand specimen using a dentist drill, making certain to obtain a representative sample and to avoid any calcite veins and/or other secondary impurities (ie. fractures).

2) An amount of the drilled sample equivalent to approximately 15 mg of pure calcite and/or dolomite was placed in one arm of a clean dry glass sample tube.

3) 4 ml of 100% H_3PO_3 was added to the other arm.

4) The tube was then evacuated.

Calcite Procedure

1) The evacuated glass sample tube was placed in a 25°C stirred water bath and allowed to equillibrate (approximately 15 minutes).

2) The sample tubes were then inverted to allow the sample and acid to mix and were left for a minimum of 16 hours (generally overnight).

Dolomite Procedure

1) Evacuated sample tubes were placed in a 50°C oven and allowed to equillibrate.

2) The sample tube were then inverted to allow the sample and acid to mix and left for a minimum if 16 hours (usually overnight).

Mixed Procedure

1) The evacuated sample tube was placed into a 25°C stirred water bath and allowed to equillibrate.

2) The sample tubes were then inverted and allowed to react for half and hour only.

3) After this half hour reaction time the CO_2 given off was extracted using the method described below.

4) This first CO_2 fraction was considered to be the calcite fraction of the sample.

5) The sample tube was then placed in a 50°C oven to react for a minimum period of 16 hours.

Collection of CO_2

1) The sample tubes were removed from the water bath/oven and connected to the vacuum line.

2) Water and any other unwanted condensibles were removed from the CO_2 by using near freezing ethanol.

3) The CO_2 was condensed by means of liquid nitrogen into a glass tube, which was then sealed with an oxy/acetylene torch.

4) The volume of gas produced from the sample, and thus the percentage yield of the sample were calculated by using the following formulas:

a) Volume(cc) = 0.0795 * CO_2 pressure

b) $\%\text{Yield (Calcite)} = \frac{\text{Volume (cc)}}{\text{Sample weight (mg)}} * 415$

c) $\%\text{Yield (Dolomite)} = \frac{\text{Volume (cc)}}{\text{Sample weight (mg)}} * 382.6$

5) This value could then be used to cross-check percentage carbonate values obtained from the Loss on Ignition analysis.

Measurement of $\partial^{13}C$

1) The purified CO_2 was then run on the Micromass 602E Isotope Mass Spectrometer to measure the isotopic ratio of the sample gas relative to the reference gas.

2) Corrections as outlined by Craig (1957) for ^{13}C and ^{18}O were automatically done by the computer.

3) Isotopic ratios were reported as Delta (∂) values ($\partial^{13}C$ and $\partial^{18}O$ respectively) relative to the PDB standard.

APPENDIX 2

HAND SPECIMEN DESCRIPTIONS

APPENDIX 2

HAND SPECIMEN DESCRIPTIONS

A977-01

Is a sample of the Wearing Dolomite from North Goddard. It is pale, light brown in fresh surface, and dark brown in weathered surface.

Many very thin calcite veins occur in the sample, which also has minor fracturing. These fractures and veins were avoided when sampling.

Malachite staining is abundant, although no sulphide crystals could be seen in fresh surface.

Occasional fine quartz grains can be found in the very fine dolomite.

A977-02

Is a sample of a massive, fine grained, dark purple, calcareous sandstone.

The sample shows no internal sedimentary structures and is approximately 6 cm thick.

The sample was situated in between parallel bedded, slightly calcareous, purple shales.

A977-03

Is a fine grained, 1.5 cm thick bed of purple limestone.

Minor laminations are present in the bottom 0.5 cm, but these are widely spaced. The sample shows no other internal structures.

This sample is also situated in between finely parallel laminated, slightly calcareous, purple shales.

A977-04

Is a dark grey limestone sample approximately 30 cm thick.

The sample is homogeneous, with the exception of widely spaced, but very faint, laminations are present. These vary from 2-6 mm spacing.

Contains framboidal chalcopyrite. The spherule is approximately 3 mm in diameter and consists of an aggregation of fine chalcopyrite grains. Other smaller concentrations of chalcopyrite, and some isolated single grains, are also present.

A977-05

Rhythmically interbedded green, calcareous shale and fine, grey limestone beds.

Load casts, scour surfaces and flutes marks present.

Limestone beds contain a few minor laminations, but is otherwise homogeneous.

A977-06

Limestone sample with darker bed overlying what appears to be HCS in finer limestone bed below.

Both limestone beds are fine grained.

A977-07

Sample of a grey, slightly sandy fine grained limestone.

Sample is massive, showing no internal sedimentary structures, and homogeneous.

A977-08

Sample of a dark, fine grained, slightly sandy limestone.

Massive 6 cm bed, no internal structure, showing minor fracturing with associated weathering.

A977-09

Light grey, very homogeneous and fine grained, sandy limestone.

Massive bed showing no apparent weathering or alteration.

A977-10

Dark, massive bed of slightly sandy limestone.

Very homogeneous.

Gives off faint H_2S odour when reacted with acid.

Has one minor and very thin calcite vein which was easily avoided when sampling.

A977-11

Limestone sample comprising alternating layers of dark grey limestone with light brown, more sandy layers.

A977-30

Cupriferous, green, fine grained dolomite.

Shale component present, thin layers of shaley dolomite at top and bottom of hand sample.

Bed is 6 cm thick.

Different in appearance from North Goddard Wearing Dolomite, but assumed to be equivalent.

Sample has no manganese weathering, and has weathered brown.

A977-31

Green limestone sample.

Sample consists of thin, faint layers of a dark and slightly lighter green limestone.

Specimen is 5 cm thick.

A977-32

5cm thick bed of limestone.

Consists of two grey limestone layers (1-1.5cm thick) separated by a very fine green silty layer, and underlain by an olive green 1.5-2cm thick limestone that contains dark flecks.

Sample appears to have very fine, only just visible, plebs of galena

Sample gives off slight H_2S smell when reacted with HCl acid.

A977-33

Massive dark fine grained limestone.

No visible internal structure or bedding.

Bed is 10 cm thick.

Gives off slight H_2S smell when reacted with acid.

A977-34

Very dark, massive limestone

One calcite vein, 1mm across, passing down far side of sample

Faint light and dark banding visible (on mm scale) in clean, wet surface.

Fine grained with minor quartz component.

A977-35

Dark, slightly sandy limestone.

Thin bed of limestone, roughly 5-7cm thick, interbedded with thin beds of shale.

No internal structure to limestone bed.

A977-36

Sample from trace fossil horizon (Palaoepaschicnius).

Finely interbedded fine sandy limestone and shaley limestone beds.

Dark limestone beds have greener beds interbedded.

No internal sedimentary structure to the beds.

A977-37

Dark limestone sample.

Sample comprises two limestone beds which are separated by a wavy and irregular dark brown dolomite banding.

Appears very recrystallized and is relatively coarse.

A977-38

Very recrystallized, dark limestone.

Very minor calcite vein running through sample.

Slightly coarser grains of calcite (fine-medium) with fine grains of quartz.

No apparent sedimentary structures.

A977-39

Recrystallized, dark limestone.

Many small calcite veins running through sample.

Small, coarse brown grains of unkown origin scattered throughout.

A977-40

Dark limestone sample.

Appears relatively recrystallized, with coarse, dark crystals present.

Light brown, irregular and discontinuous layers and specs present. Possilbly dolomite layers.

A977-41

Dark, recrystallized limestone with brown clast-like material, possibly dolomite clasts, if so then sample was possibly an intraformational conglomerate before recrystallization.

Calcite vein 1-2mm thick present in sample.

A977-70

5cm bed of dark, massive, slightly sandy limestone.

Has little internal structure, possible slight parallel lamination (bedded).

Very homogeneous.

Sharp uneven base and top surfaces into next bed.

A977-71

Very homogeneous, dark slightly sandy limestone.

Massive, no internal sedimentary structures.

Overlain onto a wavy bedded surface.

10cm thick.

A977-72

Massive, sandy limestone sample.

No internal sedimentary structures.

9cm thick bed.

A977-73

Limestone with light and dark banding.

Low angle truncations present, show evidence for fast flow regime.

Below is parallel laminated beds (showing very fast flow regime).

Sharp base and top transition into next beds, although once again is uneven.

A977-74

Light grey, slightly sandy limestone.

Massive bed with no internal structure.

Dark flecks present in sample.

Very homogeneous bed which is 10 cm thick.

Sharp base and top that are wavy bedded.

A977-55

Pale grey, slightly sandy limestone.

No internal structure on fresh surface.

Sharp base and top, direct and clean transition into green shale.

Weathered surface shows outline of internal sedimentary structures.

Base has climbing ripples, which appear to be outlined by very thin shaley layers.

This set of climbing ripples is truncated by a second set of climbing ripples.

This is followed by parallel laminations, which occur up until the top of the bed, which is approximately 15-2-cm thick.

Fine grained limestone layers which are very homogeneous.

APPENDIX 3

THIN SECTION DESCRIPTIONS

APPENDIX 3

THIN SECTION DESCRIPTIONS

Thin sections were examined under a petrological microscope. The classification used was based on Folk's limestone classification system, with the addition of one extra class, microsparite (see below). All thin sections were examined to determine the relative percentages of constituents and also to determine the amount, if any, of diagenesis and/or fluid movement the rock has experienced.

Classification:

Limestones with no allochem component:

Micrite: Indeterminable crystals and/or grains, <5μ diameter.

Microsparite: Crystal sizes that range from 5 to 30μ.

Sparite: Crystal sizes over 30μ in diameter.

Limestones with allochem component:

If the limestone contains a major proportion of intraclasts, then the prefix "Intra-" is added to Sparite or Micrite.

If the limestone is ooilitic, then the prefix "Oo-" is added.

If the limestone contains pellets and/or peloids, then the prefix "Pel-" is added.

All classification names refer to the principal carbonate constituent of the individual samples and, unless otherwise stated, refer to magnesian calcite.

A977-01

Classification: Microspar Dolomite

Location: North Goddard, Basal Unit.

General: Wearing Dolomite. Fine grained, light brown, cupriferous dolomite.

Components:

1) Dolomite 95%

2) Muscovite <1%

3) Quartz 1%

4) Plagioclase 2%

5) Opaques 1-2%

Description: Quartz, plagioclase and calcite occur as fracture fill in minor fractures. Only a very minor portion of quartz, and no plagioclase or calcite, is seen outside of these fractures. Euhedral to subhedral opaques are randomly scattered throughout sample.

A977-02

Classification: Calcareous Sandstone

Location: North Goddard, 10m.

General: Fine grained, reasonably well sorted calcareous sandstone.

Components:

1) Quartz 60%

2) Opaques 10-15%

3) Calcite 5%

4) Dolomite 5%

5) Muscovite 10-15%

6) Chlorite 2%

Description: Quartz grains are sub-rounded to rounded, and reasonably well sorted, with average grain size being roughly 50μ. Calcite is minor, and micritic. Muscovite and elongate opaque minerals, are bedding plane orientated.

A977-03

Classification: Microsparite

Location: North Goddard, 145m.

General: Slightly sandy, faintly bedded, very fine grained limestone.

Components:

1) Calcite 65-70%

2) Quartz 10-15%

3) Plagioclase 5%

4) Muscovite <5%

5) Chlorite <2%

Description: Quartz grains are reasonably sorted, ranging up to 100μ, averaging 30-40μ, and angular to subangular. Plagioclase is angular, and grains vary up to 50μ in diameter.

A977-04

Classification: Microsparite

Location: North Goddard, 375m.

General: Equigranular, carbonate rich, sulphide bearing limestone.

Components:

1) Calcite 65-70%

2) Quartz 20%

3) Plagioclase 3%

4) Pyrite 2-3%

5) Chlorite <1%

6) Muscovite 1%

Description: Framboidal pyrite present, which consists of concentrations of equigranular, euhedral crystals of pyrite. Quartz grains (25-30μ) are subrounded and are scattered through sample. Larger Quartz grains are exclusively associated with intraclasts of ferroan calcite, some of which also contain angular grains of plagioclase. The sparry calcite in these intraclasts is slightly coarser. Clasts are up to 0.5 mm long and range from elongate to round. One minor calcite vein is seen in the thin section, which has some minor pyrite mineralization associated with it.

A977-05

Classification: Microsparite

Location: North Goddard, 465m.

General: Relatively pure microspar limestone with fine grained quartz component.

Components:

1) Calcite 65-70%

2) Quartz 15-20%

3) Micritic component 10%

4) Muscovite 3%

5) Opaques 2-3%

6) Chlorite <1%

7) Plagioclase <2%

Description: Bedding plane orientated opaques and muscovite. Micro-bedding formed by micritic component of rock. Quartz grains range from 50-90μ.

A977-06

Classification: Microsparite

Location: North Goddard, 545m.

General: Fine grained microsparite limestone with minor, fine grained, quartz and plagioclase bedding.

Components:

1) Calcite 65%

2) Quartz 15-20%

3) Plagioclase 5-10%

4) Muscovite 4%

5) Chlorite 1%

6) Opaques <3%

Description: Minor calcite fracturing (0.8 mm diameter) in sample. Layers of poorly sorted (grains up to 50μ), angular to subangular, quartz and plagioclase grains define microbedding.

A977-55

Classification: Microsparite

Location: North Goddard, 630m.

General: Slightly sandy microsparitic limestone with micro-beds of quartz.

Components:

1) Calcite 55%

2) Quartz 40%

3) Plagioclase <5%

4) Muscovite 1%

Description: Sparry calcite is present but circular patches of micrite are also seen. Quartz is angular and defines the microbedding of the thin section, some grains are sutured together. Bedding is parallel laminated at the bottom and a single set of small climbing ripples is present at the top.

A977-07

Classification: Micrite

Location: North Goddard, 680m.

General: Micritic limestone.

Components:

1) Calcite ?%

2) Dolomite ?%

3) Muscovite 10%

4) Opaques 5%

Description: Sample is too fine to distinguish individual calcite and/or dolomite grains. Possible stylolytic fabric. Only muscovite and opaques are discernable, both of which are bedding plane orientated. Roughly equal portions of dolomite and calcite are present, as determined by XRD sample analysis.

A977-08

Classification: Micrite

Location: North Goddard, 730m.

General: Micritic, partially dolomitized, limestone with fine quartz component.

Components:

1) Calcite 50-55%
2) Quartz 25%
3) Dolomite 5-7%
4) Plagioclase 5%
5) Muscovite <3%
6) Opaques <5%

Description: Micritic calcite component such that grains cannot be distinguished. Dolomite rhombs, roughly 20μ, can be seen. Quartz grains are roughly 20-30μ and vary from sub-rounded to sub-angular. Some minor overgrowths can be seen on the quartz.

A977-09

Classification: Microsparite

Location: North Goddard, 946m.

General: Fine grained, slightly sandy, limestone.

Components:

1) Calcite 75%
2) Quartz 15-20%
3) Opaques 3-5%
4) Plagioclase 1-2%

Description: Angular plagioclase, up to 200μ diameter, present. Large overgrowths seen on many Plagioclase grains, some more minor overgrowthing seen on some quartz grains (Locations 1-4). Micritized, circular outlines of of iron oxide around calcite that appear to represent totally recrystallized ooids or peloids.

A977-10

Classification: Sparite

Location: North Goddard, 965m.

General: Stylolytic, fine grained, sandy limestone.

Components:

1) Calcite 25-30%
2) Quartz 45-50%
3) Micritic material 10-15%
4) Muscovite 2%
5) Plagioclase 2%
6) Opaques 2%

Description: Occasional peloid-like structure, 60-70μ diameter, which are outlined by micritic envelopes, are present. Some stylolytic fabric present, comprising the micritic component of the rock.

A977-11

Classification: Microsparite

Location: North Goddard, 985m.

General: Sparry, partially dolomitized, limestone with micro beds of fine grained quartz and plagioclase.

Components:

1) Calcite 55-60%

2) Quartz 20%

3) Micritic material 10%

4) Opaques 3%

5) Muscovite 2-3%

6) Plagioclase <2%

Description: Laminations defined by quartz and plagioclase rich layers, approximately 200μ thick, separating micritic layers and calcite rich layers. Quartz grains are angular to sub-rounded and reasonably sorted. Muscovite grains are randomly distributed and show no orientation to bedding. Micro-faulting evident in slide, seen as a micro listric extensional fault with a vertical displacement of roughly 3mm.

A977-30

Classification: Micritic Dolomite

Location: Black Range, Basal Unit.

General: Micritic dolomite layer within two shale layers.

Components:

1) Micritic dolomite component 90-95%

2) Quartz 2%

3) Muscovite <2%

4) Plagioclase 1%

Description: Some quartz and plagioclase grains sutured together. Muscovite is minor and shows no orientation to bedding. Any further description not possible due to micritic nature of sample.

A977-31

Classification: Microsparite

Location: Black Range, 130m.

General: Fine grained limestone with minor quartz and micrite component.

Components:

1) Calcite 50-55%
2) Quartz 20%
3) Muscovite 5%
4) Opaques 5%
5) Micritic component 10%
6) Plagioclase 2%
7) Dolomite 2%

Description: Muscovite is bedding plane orientated, quartz grains, up to 35μ diameter, are angular to subrounded. Rare dolomite rhombs are present. Calcite in sample is equigranular.

A977-32

Classification: Sparite

Location: Black Range, 202m.

General: Fine grained, relatively well sorted, sandy limestone, with occasional silty layer.

Components:

1) Calcite 40%
2) Quartz 40%
3) Plagioclase 5%

4) Muscovite 5-10%

5) Micritic (silty) component 3%

6) Dolomite 3-5%

7) Opaques <2%

Description: Cement made of ferroan calcite with crystal approximately 40μ diameter. Occasional dolomite rhombs 35-40μ diameter present. Muscovite is bedding plane orientated. Quartz grains are relatively well sorted, angular and up to 90μ diameter. Occasional quartz grains are sutured together. Plagioclase grains are angular and generally 20-30μ diameter, although there are occasional 70μ grains.

A977-33

Classification: Microsparite

Location: Black Range, 300m.

General: Stylolytic microsparitic, partially dolomitized limestone with minor quartz and plagioclase component.

Components:

1) Calcite 50%

2) Micritic component (clays etc) 20-25%

3) Quartz 10%

4) Dolomite 3%

5) Opaques 2-3%

Description: Stylolitic texture present as 'chicken wire' fabric, therefore not a true stylolitic fabric. Possibility that rock remained a closed system during recrystallization, and fabric is formed from growing spheres of calcite pushing clays and silts to outer.

A977-34

Classification: Micrite

Location: Black Range, 416m.

General: Micritic limestone with occasional intraclasts.

Components:

1) Opaques 10-15%

2) Intraclasts 1-2%

3) Micritic material 85%

4) Other minerals present, as determined from XRD, include: Muscovite, Quartz, Chlorite and Plagioclase.

Description: Clasts of ferroan calcite, encased in dolomite (?), ranging up to 2mm long and elongate, to 0.1mm and round are present. The calcite in these intraclasts is relatively coarser, on the boundary of microsparite and sparite. Distinguishing the percentages of any other minerals is impossible due to the micritic nature of the sample.

A977-70

Classification: Calcareous, silty sandstone

Location: Black Range, 448m.

General: Very fine grained, calcareous silty sandstone.

Components:

1) Quartz 40%

2) Calcite 20-25%

3) Silty and micritic component 20%

4) Muscovite 5-10%

5) Opaques 5-10%

Description: Muscovite and elongate opaques are bedding plane orientated. Quartz is very fine grained and angular to sub-rounded.

A977-71

Classification: Microsparite

Location: Black Range, 467m.

General: Very fine grained sandy limestone with very minor, opaque defined, laminations.

Components:

1) Quartz 40%
2) Calcite 40%
3) Muscovite and opaques 10%
4) Dolomite 5-10%
5) Plagioclase <5%

Description: Microsparitic to micritic calcite cement with bedding plane orientated muscovite and opaques. Quartz is very fine grained and sub-angular to sub-rounded.

A977-35

Classification: Micrite

Location: Black Range, 448m.

General: Micritic, slightly sandy limestone with minor dolomite component.

Components:

1) Micritic material 50-55%
2) Quartz 15%
3) Muscovite 10-15%

4) Opaques 5-10%

5) Chlorite 5%

6) Plagioclase <3%

Description: Muscovite and elongate opaques are bedding plane orientated. Quartz grains are not well sorted (ranging from 30-130μ, average 70μ) and are sub-rounded to sub-angular. Plagioclase grains are angular to sub-rounded and up to 175μ diameter.

A977-74

Classification: Microsparite

Location: Black Range, 534m.

General: Very sandy limestone with minor micritic component.

Components:

1) Calcite 30-35%

2) Quartz 20-25%

3) Chlorite 5-10%

4) Dolomite 5-10%

5) Micritic component 5%

6) Plagioclase 5%

7) Opaques and Muscovite <7%

Description: Very fine grained, absolute percentages difficult to determine.Plagioclase and quartz grains vary in size and show major overgrowthing. Plagioclase grains were originally rounded, then with overgrowth went angular.

Location 1: Overgrowthing

Location 2: Original rhomb grain with overgrowth.

A977-72

Classification: Sparite

Location: Black Range, 576m.

General: Recrystallized and double cemented, fine to coarse sparry limestone with minor microcline and quartz component.

Components:

1) Calcite 75-80%

2) Quartz 10-15%

3) Plagioclase 5-10%

4) Opaques 5%

Description: Quartz grains show major overgrowthing, as do plagioclase grains. Overgrowths on quartz grains up to 300μ are seen. The sample has experienced a similar history as A977-37, with two cementation stages being evident, the first involving fine, sparry, magnesian calcite, and the second involving coarser ferroan calcite.

Location 1 and 2: Angular plagioclase grains with major overgrowthing.

Location 3: Overgrowth on a plagioclase which is sutured to quartz.

Location 4: Ferroan calcite spars with magnesian calcite cores.

A977-36

Classification: Microsparite

Location: Black Range, 600m.

General: Very fine grained sandy limestone with a well sorted quartz component.

Components:

1) Calcite 50%

2) Quartz 30-35%

3) Micritic component 10-15%

4) Opaques 2-3%

5) Muscovite 1%

Description: Both ferroan and normal calcite present as micorsparite cement. Quartz grains are well sorted and sub-rounded to rounded.

A977-37

Classification: Intrasparite

Location: Black Range, 623m.

General: Recrystallized limestone, relatively coarse calcite, with minor quartz component.

Components:

1) Intraclasts 60% made of:

a) Sparry ferroan calcite 90-95%

b) Carbonate mud flakes 5-10%

2) Calcite cements 30%

3) Quartz 10%

4) Opaques 3%

Description: Ferroan, sparry calcite clasts, which can contain, or are simply, totally recrystallized ooids and peloids. Occasional carbonate mud flakes are present. All clasts are surrounded by a coarse, fibrous fringe of magnesian calcite. These needle-like crystals protrude into what would have been a void. Where clasts are close together, a microspar, or sparry, cement has formed. This cementation stage was followed by a second cementation period, which formed a sparry, ferroan calcite cement in the void spaces not

filled from the first cementation process. Crystal size associated with this second cementation increases towards the centre of what would have been the voids, becoming coarse in the centre of big voids. Quartz occurs in most clasts, and also as isolated grains in the cements (with cements forming around it). Many quartz grains show overgrowths.

Locations 1 & 2: Photograph under CL quartz overgrowth.

Location 3: Looks like quartz being replaced by calcite.

Location 4: Plagioclase overgrowth with calcite replacement.

A977-73

Classification: Microsparite

Location: Black Range, 684m.

General: Fine grained, microsparitic, stylolytic, sandy limestone.

Components:

1) Calcite 50%

2) Quartz 40%

3) Peloids/Ooids 5%

4) Plagioclase 5%

Description: Occasional sutured grain of quartz,but not major overgrowthing is seen. Quartz and plagioclase grains are sub-rounded to sub-angular. Stylolytic banding is present, defining areas of more micritic sparry calcite and separating more quartz rich layers.

Location 1: Big, radial ooid.

A977-38

Classification: Sparite

Location: Black Range, 689m.

General: Recrystallized, relatively coarse limestone with minor quartz component.

Components:

1) Calcite 85% made of:

   a) Clasts 60%

   b) Cements 40%

2) Quartz 10%

3) Dolomite 5%

Description: Calcite crystals range from microspar(minor) to sparite, to very coarse recrystallized calcite crystals. Quartz grains show major overgrowths. Occasional dolomite rhombs are seen.

Location 1: Dolomite rhomb in Quartz crystal

Location 2: Major quartz overgrowth,with strange striations.

Location 3: Calcite crystal with twinning on the inside, but not on outside.

A977-39

Classification: Pelsparite/Oosparite

Location: Black Range, 739m.

General: Coarse grained, recrystallized, peloid and ooid, slightly sandy limestone.

Components:

1) Coarse grained calcite 60-65%

2) Sparry calcite cement 15%

3) Ooids and Peloids 10%

4) Quartz 5-10%

5) Carbonate mud flakes 5%

6) Dolomite and Plagioclase <5%

Description: Recrystallized ooids are common, as are peloids. Differentiation is often difficult and both occur in roughly the same proportions.Coarse grained, recrystallized calcite grains have micritic rims. Quartz grains show major overgrowths, and were originally rounded to sub-rounded, averaging 100μ in diameter and well sorted. Ooids are up to 180μ, peloids up to 400μ and are elongate and oval shaped. Carbonate mud flakes are present and occur up to 1mm long. Minor stylotization is present.

Location 1: Broken ooid in micritic clast

Location 2: Over growth on quartz grain with strange striations

Location 3: Ooid with rounded quartz centre, beside a calcite vein.

Location 4: Major overgrowth on quartz.

Location 5: Euhedral quartz with ingrowth.

Location 6: Very circular structures, one calcite, onbe micritic.

A977-40

Classification: Intrasparite

Location: Black Range, 754m.

General: Recrystallized, muddy, sparry, intraclastic limestone.

Components:

1) Clasts 60% which comprise:

a) Mud flakes 20%

b) Coarse calcite in mud matrix 1%

c) Single coarse calcite crystal 60-70%

d) Recrystallized ooid, peloid, circular structure 10%

2) Quartz 5%

3) Mud layers and flakes 15-20%

4) Peloids 5%

5) Sparry cement 15-20%

Description: Quartz grains are well rounded and up to 500μ. All clasts have a micritic envelope. Calcite crystals are up to 1mm in diameter. Large, rounded intraclasts are present.

Location 1: Rounded intraclast with mud flakes

Location 2: Rounded plag/qtz with # inside:

APPENDIX 4

XRD PETROGRAPHY

APPENDIX 4

XRD MINERAOLOGY

A977-01

-Muscovite
-Qtz
-Plagioclase (Albite)
-Dolomite

A977-02

-Muscovite
-Chlorite
-Qtz
-Plagioclase (Albite)
-Equal proportions of Calcite and Dolomite

A977-03

-Muscovite
-Chlorite
-Qtz
-Plagioclase (Albite)
-Calcite (no Dolomite)

A977-04

-minor Chlorite
-possible mica
-Qtz
-Calcite (no Dolomite)
-Pyrite
-Minor Plagioclase(Albite)

A977-05

-muscovite
-chlorite
-Qtz
-Plagioclase (Albite)
-Calcite
-minimal Dolomite

A977-06

-Muscovite
-Chlorite (in same propotion as Plagioclase (Albite))
-Plagioclase (Albite)
-Qtz

-Calcite
-no Dolomite

A977-07

-Muscovite
-Chlorite
-Qtz
-Plagioclase (Albite)
-Equal proportions of Calcite and Dolomite

A977-08

-Muscovite
-Chlorite
-Qtz
-Plagioclase (Albite)
-Calcite
-some Dolomite

A977-09

-Qtz
-Calcite

A977-10

-Chlorite
-Muscovite
-Qtz
-Plagioclase (Albite)
-Calcite
-Dolomite (less than Calcite)

A977-11

-Qtz
-Calcite
-Minor dolomite
-Minor plagioclase(Albite)

A977-30

-Muscovite
-Chlorite
-Qtz
-Plagioclase (Albite)
-Dolomite

A977-31

-Muscovite
-Chlorite
-Qtz
-Plagioclase (Albite)
-Calcite
-Dolomite (minor)

A977-32

-Muscovite
-Chlorite
-Qtz
-Plagioclase (Albite)
-Calcite
-Dolomite

A977-33

-Chlorite
-Tiny bit of Muscovite
-Qtz
-Plagioclase (Albite)
-Calcite
-Minor Dolomite

A977-34

-Muscovite
-Qtz
-Chlorite
-Plagioclase (Albite)
-Calcite
-Dolomite (minor)

A977-35

-Muscovite
-Chlorite
-Qtz
-Plagioclase (Albite)
-Calcite
-Dolomite (minor)

A977-36

-Qtz
-Calcite
-Plagioclase(Albite)

A977-37

-Qtz
-Calcite

A977-38

-Qtz
-Calcite
-Very minor Dolomite

A977-39

-Qtz (minor)
-Very minor Dolomite and Plagioclase (Albite)
-Calcite (major)

A977-40

-Calcite

-Qtz(minor)
-Dolomite(minor)
-Plagioclase(minor)

A977-55

-Qtz
-Calcite

A977-70

-Muscovite
-Chlorite
-Qtz
-Calcite
-Dolomite
-Plagioclase

A977-71

-Muscovite
-Chlorite
-Qtz
-Calcite
-Dolomite
-Plagioclase

A977-72

-Qtz
-Calcite
-Microcline

A977-73

-Qtz
-Calcite
-Plagioclase

A977-74

-Qtz
-Microcline
-Muscovite
-Calcite
-Dolomite

APPENDIX 5

GEOCHEMICAL ANALYSIS

	A	B	C	D	E	F	G	H	I	J
1	NORTH GODDARD									
2	SAMPLE NO	METERAGE	Fe ppm	Mn ppm	Rb ppm	Mg ppm	Ca ppm	Sr ppm	Mn/Sr	Ca/Sr
3	977-01	0	836.6	7206.8	0	102443	234849	149	48.450	1576
4	977-02	10	18277.3	11344.5	0	73950	399790	462	24.550	865
5	977-03	145	553.7	3454.4	0	4132	437450	231	14.695	1894
6	977-04	375	1169.3	1247.5	0	4182	470583	1138	1.096	414
7	977-05	465	1253.1	748.8	0	3782	424539	5228	0.143	81
8	977-06	545	1421.8	678.0	0	3352	497853	2736	0.248	182
9	977-55	630	667.7	1082.6	0	9919	455280	1309	0.827	348
10	977-07	680	3606.1	4091.5	0	77670	421914	517	7.920	816
11	977-08	730	910.5	2477.9	0	37679	462890	659	3.760	702
12	977-09	946	350.1	249.4	0	2972	365470	239	1.040	1530
13	977-10	965	1616.2	803.0	0	52323	119546	68	11.770	1758
14	977-11	985	610.1	231.4	0	1307	419673	269	0.860	1560
15	BLACK RANGE									
16	977-30	0	14459.1	10448.5	0	35567	1013193	92	5.740	11073
17	977-31	130	1112.8	1825.6	0	18334	424393	394	4.630	1077
18	977-32	202	1396.1	1653.2	0	15780	413090	1550	1.066	267
19	977-33	300	1892.2	991.0	0	8852	457087	2794	0.355	164
20	977-34	416	2559.2	1368.0	0	18330	387870	993	1.378	391
21	977-70	448	4485.5	1562.0	0	57467	343482	351	4.450	979
22	977-71	467	1195.0	915.4	0	29195	369612	582	1.574	635
23	977-35	483	4081.6	2498.2	0	24771	372695	433	5.770	861
24	977-74	534	600.4	2456.9	0	47593	342619	343	7.160	999
25	977-72	576	627.4	2767.0	0	4005	453592	567	4.880	800
26	977-36	600	2284.8	2027.4	0	4537	466130	621	3.260	751
27	977-37	623	1278.0	892.3	0	3857	500267	381	2.340	1313
28	977-73	684	1103.6	730.1	0	15552	440373	280	2.810	1573
29	977-38	689	633.3	190.1	0	5984	466164	172	1.100	2710
30	977-39	739	1205.1	373.1	0	7624	462526	203	1.840	2278
31	977-40	754	2004.7	386.8	0	8073	459434	208	1.860	2209

	K	L	M	N	O	P	Q	R	S	T	U
1					CALCITE	CALCITE	DOLOMITE	DOLOMITE			
2	SAMPLE NO.	LOI %CARB	% YIELD	% DOLOMITE	DELTA 13C	DELTA 18O	DELTA 13C	DELTA 18O	SR ISOTOPES	SAMPLE NO.	
3	977-01	36.359	82.70	95			-0.079	-9.344		977-01	
4	977-02	6.335	9.52	50	-6.406	-14.85	-3.84	-12.257		977-02	
5	977-03	27.829	61.95	0	-8.96	-15.932				977-03	
6	977-04	33.841	70.30	0	-7.538	-15.042				977-04	
7	977-05	29.561	65.04	0	-6.434	-14.728				977-05	
8	977-06	28.146	53.10	0	-6.041	-13.362				977-06	
9	977-55	39.957	82.67	0	-5.157	-14.678			0.709676	977-55	
10	977-07	18.289	28.84	50	-4.814	-14.338	-4.847	-10.819		977-07	
11	977-08	24.104	50.85	33	-1.176	-15.062	-1.809	-11.663		977-08	
12	977-09	37.989	39.70	0	-3.25	-9.789			0.709592	977-09	
13	977-10	20.973	39.60	0	1.705	-10.135				977-10	
14	977-11	35.84	79.50	0	-1.134	-8.415				977-11	
15											
16	977-30	12.142	18.95	95	-1.69	-9.27				977-30	
17	977-31	24.164	51.49	18	-7.549	-14.882	-6.902	-13.523		977-31	
18	977-32	23.287	50.57	13	-6.295	-14.202	-5.88	-12.852		977-32	
19	977-33	29.191	62.36	0	-6.944	-14.145				977-33	
20	977-34	17.589	36.77	14	-6.138	-14.658	-5.096	-6.931		977-34	
21	977-70	19.325	37.90	45	-6.303	-13.357	-5.84	-10.076		977-70	
22	977-71	25.359	53.64	30	-4.91	-14.65	-5.193	-11.347		977-71	
23	977-35	14.811	28.42	23	-3.944	-13.415	-3.479	-10.457		977-35	
24	977-74	25.016	50.47	35	-1.857	-14.127	-3.07	-10.243		977-74	
25	977-72	38.396	82.40	0	4.669	-14.301				977-72	
26	977-36	39.957	62.15	0	2.886	-13.636				977-36	
27	977-37	41.096	86.07	0	4.53	-13.219			0.709359	977-37	
28	977-73	30.576	58.90	5	3.439	-12.35				977-73	
29	977-38	41.462	88.90	0	3.541	-12.034			0.71001393	977-38	
30	977-39	41.308	86.30	0	6.611	-11.855				977-39	
31	977-40	41.23	84.80	0	6.54	-11.52			0.7102602	977-40	